JAPANESE DERMATOLOGICAL ASSOCIATION
THE JOURNAL OF DERMATOLOGY

doi: 10.1111/1346-8138.12420

Journal of Dermatology 2014; **41**: 340–342

CONCISE COMMUNICATION

Case of *Fusarium* paronychia successfully treated with occlusive dressing of antifungal cream

Isamu IKEDA,[1] Tadashi OHNO,[2] Hideaki OHNO,[3] Yoshitsugu MIYAZAKI,[3] Katsutaro NISHIMOTO,[4] Satoshi FUKUSHIMA,[5] Takamitsu MAKINO,[5] Hiromobu IHN[5]

Departments of [1]Dermatology and [2]Bacteriology, Omuta Tenryo Hospital, Fukuoka, [3]Department of Chemotherapy and Mycoses, National Institute of Infectious Diseases, Tokyo, [4]Department of Dermatology, Nagasaki Ekisaikai Hospital, Nagasaki, and [5]Faulty of Life Sciences, Department of Dermatology and Plastic Surgery, Kumamoto University, Kumamoto, Japan

ABSTRACT

We report a case of refractory *Fusarium* paronychia in a 42-year-old man with Behçet's disease receiving oral cyclosporin and corticosteroid. Symptoms resembling candidal paronychia of his little finger could not be cured by topical ketoconazole and oral terbinafine. The pathogen was identified as *Fusarium solani* species complex by gene analysis, and was multiple drug resistant. The case eventually resolved by occlusive dressing therapy with 0.5% amorolfine cream for 3 months.

Key words: amorolfine, *Fusarium*, multiple drug resistant, occlusive dressing therapy, topical treatment.

INTRODUCTION

The *Fusarium* species are saprophytic organisms that are widely distributed in aerial plants and soil. The organisms are known to cause local infection including onychomycosis, skin ulcer, bone and joint infections, and keratotic ulcer in immunocompetent hosts.[1–5] The *Fusarium* species are also described as important opportunistic pathogen. Rapidly progressive infection with multi-organ system involvement is distinctive in immunocompromised hosts. The prognosis is very poor despite antifungal therapy, particularly in neutropenic patients.[6–9]

We report a case of paronychia caused by *Fusarium solani* species complex in a man receiving oral cyclosporin and corticosteroid. The fungus was multiple drug resistant for systemic antifungals, but successfully treated with occlusive dressing of amorolfine cream.

CASE REPORT

A 42-year-old man with Behçet's disease receiving cyclosporin at 150 mg daily and prednisolone at 20 mg daily consulted us with a 2-week history of painful paronychia affecting the left little finger in August 2012. The patient had tried to treat the paronychia with an ointment containing betamethasone valerate and gentamycin sulfate, but it had been worsened. He had severe uveitis and spent most of his time indoors, so had no chance to touch the soil and plants.

On admission, his little finger had purulent drainage with surrounding edema and erythema. The nail plate was apparently clear and healthy, although yellowish staining was observed over the proximal area (Fig. 1a).

Direct microscopic examination of yellow-white drainage showed a fungal element of large round cells with hyaline tortuous hyphae (Fig. 1b). Culture on potato dextrose agar with chloramphenicol led to the growth of a floccose yellow-brownish colony (Fig. 1c). Microscopically, microconidia were abundant, oval, one- to two-celled and formed from long phialides (Fig. 1d). The fungus was sent to the National Institute of Infectious Diseases (Tokyo, Japan) and identified as *F. solani* species complex by gene analysis. The minimal inhibitory concentrations (MIC) were as follows: micafungin, more than 16; amphotericin B, 4; flucytosine, more than 64; fluconazole, more than 64; itraconazole, more than 8; voriconazole, 2; and posaconazole, more than 16 (μg/mL).

The patient was treated with 2% ketoconazole cream for 3 weeks, but it had no effect. Oral terbinafine at 125 mg daily was begun in August 2012, along with a survey of MIC for terbinafine. In the initial 2 weeks, he developed onycholysis (Fig. 2a), and his paronychia showed some improvement after exfoliation of the affected nail plate. Gradual regrowth of the nail plate was observed afterwards, but it was deformed and painful paronychia persisted. The therapy was continued in the expectation of further improvement, but the MIC for terbinafine was revealed to be high (>32 μg/mL) and oral terbinafine was discontinued in November 2012. Systemic therapy

Correspondence: Isamu Ikeda, M.D., Department of Dermatology, Omuta Tenryo Hospital, 1–100 Tenryo, Omuta City, Fukuoka 836-8566, Japan. Email: fs74kai@gmail.com
Received 18 October 2013; accepted 27 December 2013.

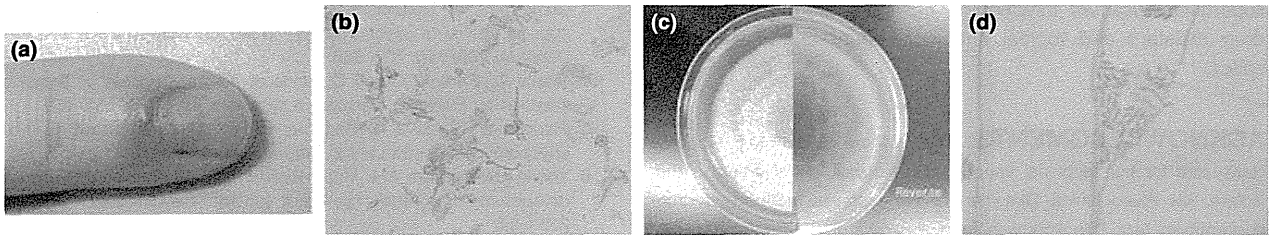

Figure 1. (a) Paronychia with proximal leukonychia was seen on admission. (b) Septate, hyaline and tortuous hyphae were observed by direct examination of paronychia (original magnification ×400). (c) Yellow-brownish colony grew on potato dextrose agar (on the 9th day). (d) Microconidia were abundant, oval, one- to two-celled and formed from long phialides (methylene blue staining, original magnification ×400).

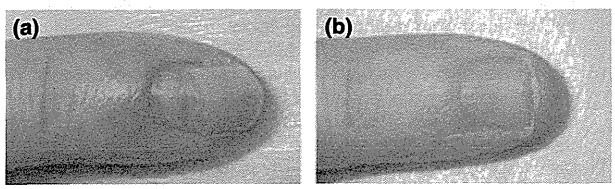

Figure 2. (a) Onycholysis was seen at the beginning of oral terbinafine. A white band was seen in the proximal area of the nail bed. (b) Normal nail plate was restored after occlusive dressing of amorolfine cream.

with voriconazole seemed adequate regarding MIC, but its use was restricted because he had severe visual impairment from Behçet's disease. He was treated with topical 1% butenafine and 1% terbinafine cream, but there was no apparent improvement.

In January 2013, direct microscopic examination revealed the presence of residual fungus and the therapy was switched to simple application of 0.5% amorolfine cream. A smooth, healthy nail plate appeared in the proximal area, but acute purulent paronychia developed again in February 2013. Direct microscopic examination and culture of the drainage showed the presence of *Fusarium*, the same strain as identified before. The therapy was switched to occlusive dressing therapy (ODT) of 0.5% amorolfine cream. The nail plate and proximal nail fold were covered with plastic wrap for 8 h/day after application of the cream.

His paronychia showed apparent improvement in 5 weeks of ODT, and was clinically cured after 12 weeks of the therapy (Fig. 2b). Direct examination as well as the culture of scales showed a negative result at the 5th and 12th weeks. His infection was completely controlled by July 2013, 5 months after the beginning of the ODT.

DISCUSSION

A recent increase in the number of non-dermatophyte filamentous fungus (NDF) infections in onychomycosis has been reported.[1–5] *Fusarium* onychomycosis mimics dermatophyte infection, but produces specific clinical findings. The form of proximal subungual onychomycosis is dominant, and it is occasionally accompanied by persisting painful eruption and induration on the perionychium.[2–5] On direct examination of *Fusarium* onychomycosis, the majority of cases exhibit irregular forms and round-shaped chlamydospore-like structure as seen in our case.[3]

As a *Fusarium* paronychia, our case showed unusual symptoms including pustulous flare-up and lack of preceding onychomycosis. A similar case of acute purulent *Fusarium* paronychia in a patient with acute myelogenous leukemia was reported by Bourgeois *et al.*[8] The patient developed disseminated *Fusarium* infection, from a toenail paronychia, without symptoms indicating pre-existing fungal infection. The unusual course of our patient may suggest a higher risk of lethal infection, so we are still paying attention to his course.

Treatment of NDF onychomycosis is not well standardized, especially in *Fusarium* infection. Standard systemic therapy with itraconazole and/or terbinafine often fails to eradicate the molds of onychomycosis.[2,10] Besides the poor outcome of systemic therapy, an advantage of topical treatment has been reported in NDF onychomycosis.[2,10] Use of ciclopirox nail lacquer and topical terbinafine with nail avulsion has been described.[2,5] Recently, the use of topical amphotericin B has been recommended.[3,10]

The strain isolated from our patient was resistant to multiple drugs including itraconazole and terbinafine. Voriconazole showed an effect, but the patient had poor vision due to severe uveitis, and its use was restricted due to the high frequency of visual disturbance as a side-effect. In consideration of the risks and benefits, we decided to retry the local treatment using a more potent drug against *F. solani* species complex. As amphotericin B cream is not available in Japan and ciclopirox was difficult to obtain, we tried amorolfine, a morpholine derivative. Generally, *Fusarium* spp. are resistant to amorolfine, with the exception of *F. solani*. De Vroey *et al.*[11] reported that 19 out of 22 *F. solani* isolates were inhibited by 1 μg/mL amorolfine. Simple application of 0.5% amorolfine cream succeeded in clearing the nail plate, but it was not sufficient to eradicate the fungus and paronychia recurred. The failure of treatment may be attributable to a lower drug concentration around the nail matrix, so we selected ODT, a classical way of permeating drugs deep under the skin. It was useful to resolve the problem.

Occlusive dressing therapy of adequate antifungal cream should be considered as an option for treating intractable

superficial *Fusarium* infection in case the fungus is multiple drug resistant and topical antifungal agent shows a limited effect.

ACKNOWLEDGMENTS: The authors thank Ms Nobuko Nakayama for her technical support of molecular identification of the isolate, Ms Akiko Ishida Okawara for her technical support of drug susceptibility test. This work was supported by a grant from the Ministry of Health, Labor and Welfare of Japan (H23-shinkou-ippan-018, H23-shinkou-ippan-007, H24-shinkou-ippan-013, H25-shinkou-ippan-006, H25-shinkou-shitei-002), Grant-in-Aid for Scientific Research (B) 21390305 from the Ministry of Education, Culture, Sports, Science and Technology of Japan.

CONFLICT OF INTEREST: None.

REFERENCES

1 Ritchie EB, Pinkerton ME. *Fusarium oxysporum* infection of the nail. *Arch Dermatol* 1959; **79**: 705–708.
2 Tosti A, Piraccini BM, Lorenzi S. Onychomycosis caused by non-dermatophytic molds: clinical features and response to treatment of 59 cases. *J Am Acad Dermatol* 2000; **42**: 217–224.
3 Guihermetti E, Takahachi G, Shinobu CS, Svidzinski TI. Fusarium spp. as agents of onychomycosis in immunocompetent hosts. *Int J Dermatol* 2007; **46**: 822–826.
4 Gianni C, Cerri A, Crosti C. Unusual clinical features of fingernail infection by *Fusarium oxysporum*. *Mycoses* 1997; **40**: 455–459.
5 Ranawaka RR, Silva N, Ragunathan RW. Non-dermatophyte mold onychomycosis in Sri Lanka. *Dermatol Online J* 2012; **18**(1): 7.
6 Young CN, Meyers AM. Opportunistic fungal infection by *Fusarium oxysporum* in a renal transplant patient. *Sabouraudia* 1979; **17**: 219–223.
7 Martino P, Gastaldi R, Raccah R, Girmenia C. Clinical pattern of *Fusarium* infections in immunocompromised patients. *J Infect* 1994; **28**(Suppl 1): 7–15.
8 Bourgeois GP, Cafardi JA, Sellheyer K, Andea AA. Disseminated *Fusarium* infection originating from paronychia in a neutropenic patient: a case report and review of the literature. *Cutis* 2010 (Apr); **85**(4): 191–194.
9 Nucci M, Aniaissie E. Cutaneous infection by Fusarium species in healthy and immunocompromised hosts: implications for diagnosis and management. *Clin Infect Dis* 2002; **35**: 902–920.
10 Baudraz-rosselet F, Ruffieux C, Lurati M, Bontems O, Monod M. Onychomycosis insensitive to systemic terbinafine and azole treatments reveals non-dermatophyte moulds as infectious agents. *Dermatology* 2010; **220**: 164–168.
11 De Vroey C, Desmet P, Li Z-Q, Mukamurangwa P, Raes-Wuytack C. Further studies on the in vitro antifungal activity of amorolfine. *Mycoses* 1996; **39**: 41–44.

Upregulation of miR-18a-5p contributes to epidermal necrolysis in severe drug eruptions

Asako Ichihara, MD, PhD,* Zhongzhi Wang, PhD,* Masatoshi Jinnin, MD, PhD, Yuki Izuno, Naoki Shimozono, PhD, Keitaro Yamane, Akihiko Fujisawa, MD, Chikako Moriya, MD, PhD, Satoshi Fukushima, MD, PhD, Yuji Inoue, MD, PhD, and Hironobu Ihn, MD, PhD *Kumamoto, Japan*

Background: Toxic epidermal necrolysis (TEN) is a severe drug-induced cutaneous reaction. Although one of the primary histologic features of TEN is keratinocyte apoptosis, its exact mechanism remains unknown.
Objectives: We investigated the role of microRNAs (miRNAs) in the pathogenesis of severe drug eruptions and evaluated the possibility that miRNA can be a disease marker.
Methods: miRNAs were extracted from tissues and sera of patients. PCR array analyses were performed to identify pathogenic miRNAs. The results were confirmed with quantitative real-time PCR, *in situ* hybridization, transient transfection of small interfering RNAs or miRNA mimics into cultured keratinocytes, flow cytometry, immunoblotting, luciferase assay, and immunohistochemistry.
Results: PCR array analysis and real-time PCR using tissue miRNAs demonstrated that the miR-18a-5p level was increased in the skin of patients with TEN *in vivo*. Transfection of the miR-18a-5p mimic into keratinocytes *in vitro* resulted in increased apoptotic cell numbers and caspase-9 activity, which were also increased in the skin of patients with TEN. The miR-18a-5p mimic also downregulated the expression of B-cell lymphoma/leukemia-2-like protein 10 (BCL2L10), an anti-intrinsic apoptotic molecule. A luciferase assay with the *BCL2L10* 3′ untranslated region showed *BCL2L10* is directly targeted by miR-18a-5p. The protein and mRNA expressions of BCL2L10 were decreased in the skin of patients with TEN. Transfection with *BCL2L10* small interfering RNA induced keratinocyte apoptosis and caspase activity. Furthermore, serum miR-18a-5p levels tended to be increased in patients with TEN and were correlated with areas of skin erythema or erosion in patients with drug eruptions.
Conclusions: Our results indicated that downregulated BCL2L10 caused by miR-18a-5p overexpression mediates intrinsic keratinocyte apoptosis in patients with TEN. Serum miR-18a-5p levels can be a useful disease marker for drug eruptions. (J Allergy Clin Immunol 2014;133:1065-74.)

Key words: *MicroRNA, apoptosis, drug eruption, keratinocyte, serum*

Abbreviations used
BCL2L10: B-cell lymphoma/leukemia-2-like protein 10
BSA: Body surface area
Ct: Cycle threshold
EM: Erythema multiforme
miRNA: MicroRNA
NHEK: Normal human epidermal keratinocyte
siRNA: Small interfering RNA
SJS: Stevens-Johnson syndrome
TEN: Toxic epidermal necrolysis
TUNEL: Terminal deoxynucleotidyl transferase-mediated dUTP nick end labeling
UTR: Untranslated region

Drug eruptions are adverse cutaneous reactions caused by drug administration. Not all drug eruptions have allergic mechanisms; some have nonallergic causes (eg, toxicity, overdose, or side effects). Allergic drug eruptions are divided into several clinical types, including maculopapular-type, lichenoid-type, and fixed drug eruptions. The erythema multiforme (EM) type is also known to be a common type of drug eruption; the minor form is mild and self-limited, whereas the major form is accompanied by systemic symptoms and sometimes becomes severe and life-threatening.

Stevens-Johnson syndrome (SJS) and toxic epidermal necrolysis (TEN) are characterized by targetoid erythematous lesions, with blistering and erosion of the skin and mucous membranes. SJS and TEN are considered 2 different severe forms of major EM. SJS involves less than 10% of the body surface area (BSA), whereas TEN affects more than 10% of the BSA. In addition, ocular, gastrointestinal, liver, renal, and respiratory involvement is sometimes observed in patients with TEN. Because of a high mortality rate, it is important to diagnose these diseases in the early stage, predict severity, and treat intensively. Histologically, the erosions of SJS and TEN result from keratinocyte apoptosis and epidermal detachment.[1,2] However, the exact mechanisms remain unknown.

MicroRNAs (miRNAs) are small noncoding RNAs only 22 nucleotides long on average.[3] miRNAs usually bind to complementary sequences in the 3′ untranslated regions (UTRs) of target mRNAs and inhibit their expression.[4,5] Because more than a thousand miRNAs have been identified in human subjects,[6] miRNAs are thought to be the most abundant class of regulators. miRNAs have been implicated in the immune response, as well as in cell development, cell differentiation, organogenesis, growth control, and apoptosis. Accordingly, many publications have demonstrated that miRNAs are involved in the pathogenesis of various human diseases, such as immunologic disorders, neurologic

From the Department of Dermatology and Plastic Surgery, Faculty of Life Sciences, Kumamoto University.
*These authors contributed equally to this work.
Disclosure of potential conflict of interest: The authors declare that they have no relevant conflicts of interest.
Received for publication September 13, 2012; revised August 21, 2013; accepted for publication September 4, 2013.
Available online November 1, 2013.
Corresponding author: Masatoshi Jinnin, MD, PhD, Department of Dermatology and Plastic Surgery, Faculty of life sciences, Kumamoto University, 1-1-1 Honjo, Kumamoto, 860-8556, Japan. E-mail: mjin@kumamoto-u.ac.jp.
0091-6749/$36.00

http://dx.doi.org/10.1016/j.jaci.2013.09.019

diseases, cardiovascular diseases, metabolic disorders, and cancers.[7-14]

Recently, several studies have indicated an association between drug eruptions and genetic factors (eg, HLA typing).[15] However, no reports have investigated the contribution of epigenetics, including miRNAs, to the pathogenesis of drug eruptions. Our study is the first to evaluate the possibility that miRNAs play a role in the pathogenesis of drug eruptions, especially TEN.

METHODS

Patient materials

Serum samples were obtained from 8 patients with TEN, 10 patients with SJS, 15 patients with EM minor, and 22 healthy volunteers. Patients with other chronic inflammatory or malignant diseases were excluded from this study. In 2 of the 8 patients with TEN, the cause of the disease was identified to be allopurinol or carbamazepine administration. In the remaining 6 patients, multiple drugs were suspected, and we were unable to identify the exact cause. In 3 of the 10 patients with SJS, phenobarbital, fosfomycin calcium, or lamotrigine administration was identified as the cause. Meanwhile, the causative drugs were unknown in the remaining 7 patients. In addition, candesartan cilexetil, carbamazepine, creosote, or interferon administration was thought to be the cause in 4 of the 15 patients with EM. Skin specimens were also obtained from 4 patients with TEN, 3 patients with SJS, 8 patients with EM minor, 4 patients with psoriasis, 4 patients with atopic dermatitis, and 6 control subjects. These samples were stored at −80°C or fixed in formaldehyde after resection. Institutional review board approval and written informed consent were obtained before the patients and healthy volunteers were entered into the study, according to the Declaration of Helsinki.

Cell culture

Normal human epidermal keratinocytes (NHEKs; Lonza, Walkersville, Md) were cultured in KBM-Gold Basal Medium with KGM-Gold Single-Quots at 37°C in 5% CO_2.

RNA isolation and quantitative real-time PCR

Total RNA isolation from paraffin-embedded tissue sections was performed with the RNeasy FFPE kit (Qiagen, Valencia, Calif). Total RNA was extracted from cultured cells by using ISOGEN (Nippon Gene, Tokyo, Japan). cDNA synthesis and real-time PCR were performed, as described previously.[16] Primers for B-cell lymphoma/leukemia-2-like protein 10 *(BCL2L10)* and glyceraldehyde-3-phosphate dehydrogenase were purchased from Takara and SABioscience (Frederick, Md), respectively.

miRNA extraction from skin tissues, cultured cells, and sera

Small RNAs were extracted from tissue sections by using the miRNeasy FFPE kit (Qiagen). miRNAs were obtained from the total RNA of cultured cells by using the RT^2 qPCR-Grade miRNA Isolation Kit (SABioscience, Qiagen). miRNA isolation from serum samples was performed with the miRNeasy RNA isolation kit (Qiagen) and synthetic nonhuman miRNA (*Caenorhabditis elegans* miR-39; Takara, Otsu, Japan), as described previously.[17-21]

miRNA PCR array

miRNAs were reverse transcribed into cDNA by using the miScript II RT Kit (Qiagen). The cDNA was mixed with QuantiTect SYBR Green PCR Master Mix, and the mixture was added to Human miFinder 384 Array (Qiagen). PCR was performed on the Bio-Rad CFX384 (Bio-Rad Laboratories, Hercules, Calif).

Real-time PCR of miRNAs

cDNA was synthesized from the miRNA by using the Mir-X miRNA First Strand Synthesis and SYBR qRT-PCR Kit (Takara). The sequences of the primers were designed based on miRBase (http://www.mirbase.org). PCR was performed, as previously described.[16] The transcript level of each miRNA was normalized to that of cel-miR-39 in serum samples or to that of U6 in other samples.

In situ hybridization

In situ hybridization was performed with 5′-locked digoxigenin-labeled nucleic acid probes complementary to human mature miR-18a-5p (Exiqon, Vedbaek, Denmark) at 59°C overnight.[16]

Transient transfection

Small interfering RNA (siRNA) against *BCL2L10* was purchased from Thermo Scientific Dharmacon (Rockford, Ill). miRNA mimics, inhibitors, and miScript Target protectors were purchased from Qiagen.

For reverse transfection, miRNA mimics, inhibitors, protectors, or siRNAs were mixed with Lipofectamine RNAiMAX (Invitrogen, Carlsbad, Calif) and then added when the cells were plated, followed by incubation at 37°C in 5% CO_2.

Luciferase reporter assay

A luciferase construct containing the *BCL2L10* 3′ UTR was purchased from GeneCopoeia (Rockville, Md). Substitution mutations of the miR-18a-5p seed match were introduced by using Quick Change site-directed mutagenesis kits (Stratagene, La Jolla, Calif) and verified by means of sequencing. miRNA mimics and reporter plasmids mixed with Lipofectamine 2000 (Invitrogen) were added when the cells were plated, followed by incubation at 37°C. The Luc-Pair miR luciferase assay (GeneCopoeia) and the FilterMax F5 microplate reader (Molecular Devices, Sunnyvale, Calif) were used to analyze luciferase expression.

Apoptosis assay

Cellular apoptosis was measured by using the terminal deoxynucleotidyl transferase-mediated dUTP nick end labeling (TUNEL) assay and the Annexin V assay with the Guava TUNEL Kit and FlowCellect Annexin Red Kit (Millipore, Temecula, Calif), respectively.[22,23]

Caspase assay

Caspase activity was determined by using the Caspase-3 Colorimetric Assay Kit and Caspase-9 Colorimetric Assay Kit (R&D Systems, Minneapolis, Minn).

Immunohistochemical staining

Immunohistochemical staining was performed with antibodies for BCL2L10 or active caspase-9 (Abcam, Cambridge, United Kingdom) overnight at 4°C, as described previously.[16]

Cell lysis and immunoblotting

NHEKs or tissue samples were washed with PBS twice and lysed in Denaturing Cell Extraction Buffer (Biosource International, Camarillo, Calif). Immunoblotting was performed with antibodies for BCL2L10, active caspase-9 (IMGENEX, San Diego, Calif), active caspase-3 (BD Bioscience, Bedford, Mass), or β-actin (Santa Cruz Biotechnology, Santa Cruz, Calif).[16]

Statistical analysis

Statistical analysis was performed with the Mann-Whitney *U* test for comparison of medians. Correlations were assessed by using Pearson correlation coefficients. *P* values of less than .05 were considered significant. In Table I, *P* values determined by using the Mann-Whitney *U* test in comparison with the values in normal skin were transformed into *q* values by using the *q* value method.[24]

TABLE I. Fifteen miRNAs significantly upregulated or downregulated in the skin of patients with TEN compared with healthy skin, as measured by using a PCR array

	Healthy skin, mean ± SD		Patients with TEN, mean ± SD		Patients with psoriasis, mean ± SD		Patients with atopic dermatitis, mean ± SD	
	P value	*q* Value	*P* value	*q* Value	*P* value	*q* Value	*P* value	*q* Value
hsa-miR-9-5p	1.00 ± 1.49		0.00 ± 0.00		0.02 ± 0.03		2.14 ± 2.83	
	—	—	.0369	0.8472	.0463	0.6189	.8273	0.8446
hsa-miR-18a-5p	1.00 ± 1.08		7.93 ± 1.11		1.75 ± 3.04		2.07 ± 3.58	
	—	—	.0495	0.8472	.5066	0.7261	.5066	0.8208
hsa-miR-29a-5p	1.00 ± 0.88		0.05 ± 0.01		0.11 ± 0.18		0.94 ± 1.16	
	—	—	.0495	0.8472	.1266	0.6189	.8273	0.8446
hsa-miR-33a-3p	0.00 ± 0.00		1.00 ± 0.75		0.01 ± 0.01		0.04 ± 0.07	
	—	—	.0369	0.8472	.1213	0.6189	.3173	0.8208
hsa-miR-191-3p	1.00 ± 0.69		0.20 ± 0.23		1.14 ± 1.25		0.75 ± 0.56	
	—	—	.0495	0.8472	.8273	0.8394	.5127	0.8208
hsa-miR-210	1.00 ± 0.30		3.09 ± 1.05		1.22 ± 1.06		0.92 ± 0.82	
	—	—	.0495	0.8472	.5127	0.7261	.8273	0.8446
hsa-miR-223-3p	1.00 ± 0.23		2.53 ± 1.37		3.40 ± 3.24		3.65 ± 0.68	
	—	—	.0495	0.8472	.5127	0.7261	.0495	0.8208
hsa-miR-298	1.00 ± 0.79		0.02 ± 0.03		0.29 ± 0.17		0.01 ± 0.01	
	—	—	.0495	0.8472	.1266	0.6189	.0495	0.8208
hsa-miR-346	1.00 ± 0.19		8.79 ± 6.19		7.92 ± 11.80		9.64 ± 5.12	
	—	—	.0495	0.8472	.5127	0.7261	.0495	0.8208
hsa-miR-378a-5p	1.00 ± 1.68		0.00 ± 0.00		0.00 ± 0.00		1.07 ± 1.23	
	—	—	.0463	0.8472	.0463	0.6189	.5127	0.8208
hsa-miR-383	1.00 ± 0.75		0.00 ± 0.00		0.14 ± 0.24		0.00 ± 0.00	
	—	—	.0369	0.8472	.1212	0.6189	.0463	0.8208
hsa-miR-424-3p	1.00 ± 1.23		0.00 ± 0.00		1.81 ± 2.78		0.05 ± 0.09	
	—	—	.0369	0.8472	.8273	0.8394	.1212	0.8208
hsa-miR-495-3p	1.00 ± 1.05		0.07 ± 0.01		11.34 ± 14.22		5.25 ± 6.92	
	—	—	.0495	0.8472	.5127	0.7261	.5127	0.8208
hsa-miR-605	1.00 ± 0.62		0.18 ± 0.12		2.78 ± 3.39		4.17 ± 6.28	
	—	—	.0495	0.8472	.5127	0.7261	.8273	0.8446
hsa-miR-1908	1.00 ± 1.28		0.04 ± 0.05		0.17 ± 0.19		1.42 ± 1.25	
	—	—	.0495	0.8472	.2752	0.6477	.8273	0.8446

The miRNA expression profile in each disease *in vivo* was evaluated by using a PCR array. The fold change was calculated as follows: $1/2^{(\text{Raw Ct of each miRNA} - \text{Mean Ct of small RNA housekeeping genes})}$.

The mean fold change (mean) and SD of each miRNA is shown. The mean value of the healthy skin samples was set at 1. When the value of healthy skin was 0, the mean value of another sample was set at 1. *P* values and *q* values compared with the values in healthy skin samples are indicated.

RESULTS

miRNA expression profile in drug eruptions

As an initial experiment, to determine which miRNAs are involved in the pathogenesis of drug eruptions, miRNAs were obtained from the skin tissues of 3 patients with TEN, and the global miRNA expression profile of skin of patients with TEN was compared with that of 3 samples of healthy skin by using a PCR array consisting of 372 miRNAs (see Table E1 in this article's Online Repository at www.jacionline.org). Three samples of the skin of patients with psoriasis and atopic skin were also included in this experiment as disease control specimens.

There were 15 miRNAs significantly upregulated or downregulated in the skin of patients with TEN compared with healthy skin, according to the array (Table I). Among them, the expression of miR-18a-5p, miR-33a-3p, and miR-210 was increased and expression of miR-495-3p was decreased in the tissues of patients with TEN significantly and specifically when compared with that seen in the skin of patients with psoriasis and atopic skin, as well as healthy skin. We confirmed the array results using quantitative real-time PCR analysis with a specific primer for each miRNA and increased number of samples (4 from patients with TEN, 3 from patients with SJS, 8 from patients with EM minor, 4 from patients with psoriasis, 4 from patients with atopic dermatitis, and 5 from healthy skin). Among the 3 upregulated or 1 downregulated miRNAs in patients with TEN, only the expression of miR-18a-5p (UAAGGUGCAUCUAGUGCAGAUAG) was still significantly upregulated in the TEN samples compared with that observed in the other patient groups, according to the real-time PCR analysis (Fig 1, *A*). Furthermore, miR-18a-5p levels in the affected skin of the patients with EM and those with SJS were increased slightly compared with those in healthy skin and lower than those in the skin of patients with TEN. These results suggest that miR-18a-5p levels are correlated with the severity of drug eruptions. Therefore we focused on miR-18a-5p, one of the miR-17-92 miRNA cluster at 13q31.3, which was previously called miR-18a and recently renamed miR-18a-5p based on miRBase. On the other hand, levels of miR-17-5p, miR-19b-3p, and miR-20a-5p, other miR-17-92 cluster members, also tended to be increased in the samples from patients with TEN compared with healthy skin according to the array, although the findings were not statistically significant (see Table E1). miR-19a-3p and miR-92a-3p were similarly expressed in healthy skin and the skin of patients with TEN. Consistently, real-time PCR revealed expression of these 5 miRNAs, and

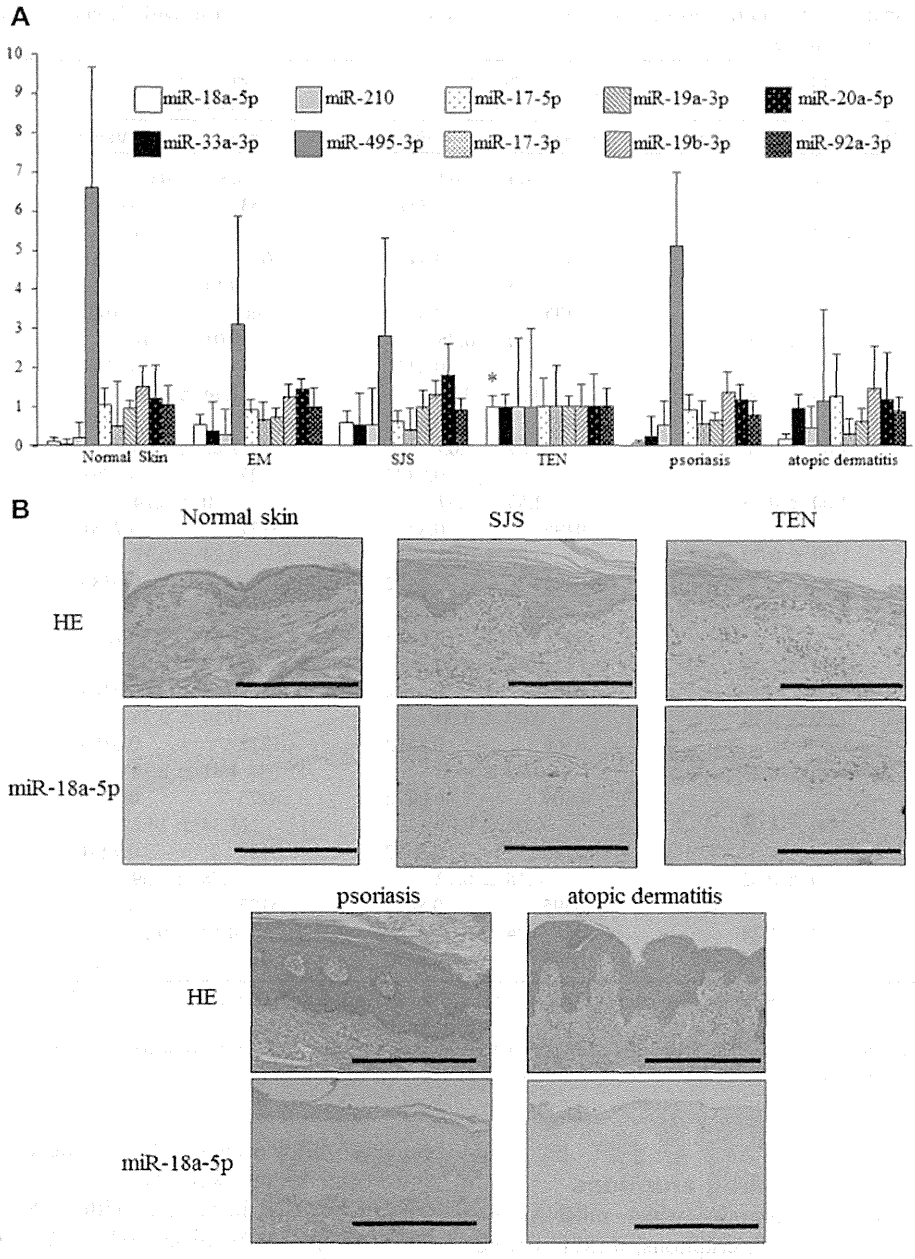

FIG 1. Expression of miR-18a-5p in cutaneous drug eruptions *in vivo*. **A,** Relative miRNA levels in tissues of 6 subjects with healthy skin, 8 patients with EM, 3 patients with SJS, 4 patients with TEN, 4 patients with psoriasis, and 4 patients with atopic dermatitis. *Error bars* represent SDs. $*P < .05$ compared with values in the other disease samples. **B,** *Upper panels,* Hematoxylin and eosin *(HE)* staining. *Bars* = 200 μm. *Lower panels, In situ* detection of miR-18a-5p. miR-18a-5p stained brown.

expression of the remaining miR-17-92 cluster member, miR-17-3p, was not significantly altered in the skin of patients with TEN compared with that seen in other patient groups (Fig 1, *A*). In addition, the array indicated expression of miR-18b-5p (UAAGGUG CAUCUAGUGCAGUUAG), which has a similar sequence to miR-18a-5p, was not different between healthy skin and skin of patients with TEN (see Table E1). Therefore the skin of patients with TEN was likely to overexpress miR-18a-5p specifically.

In situ hybridization showed that signals for miR-18a-5p were evident in the epidermis of patients with SJS and those with TEN but not in healthy skin samples (Fig 1, *B*). Of note, the miR-18a-5p signals were most apparent in the epidermal apoptotic cells of the skin of patients with SJS and skin of patients with TEN, suggesting that miR-18a-5p might contribute to keratinocyte apoptosis. miR-18a-5p expression was not found in either the skin of patients with psoriasis or atopic skin.

Downregulated BCL2L10 expression caused by miR-18a-5p overexpression is involved in keratinocyte apoptosis

We expected that miR-18a-5p might play a role in the pathogenesis of drug eruptions, especially TEN. One of the primary histologic features of TEN is keratinocyte apoptosis.[1,2]

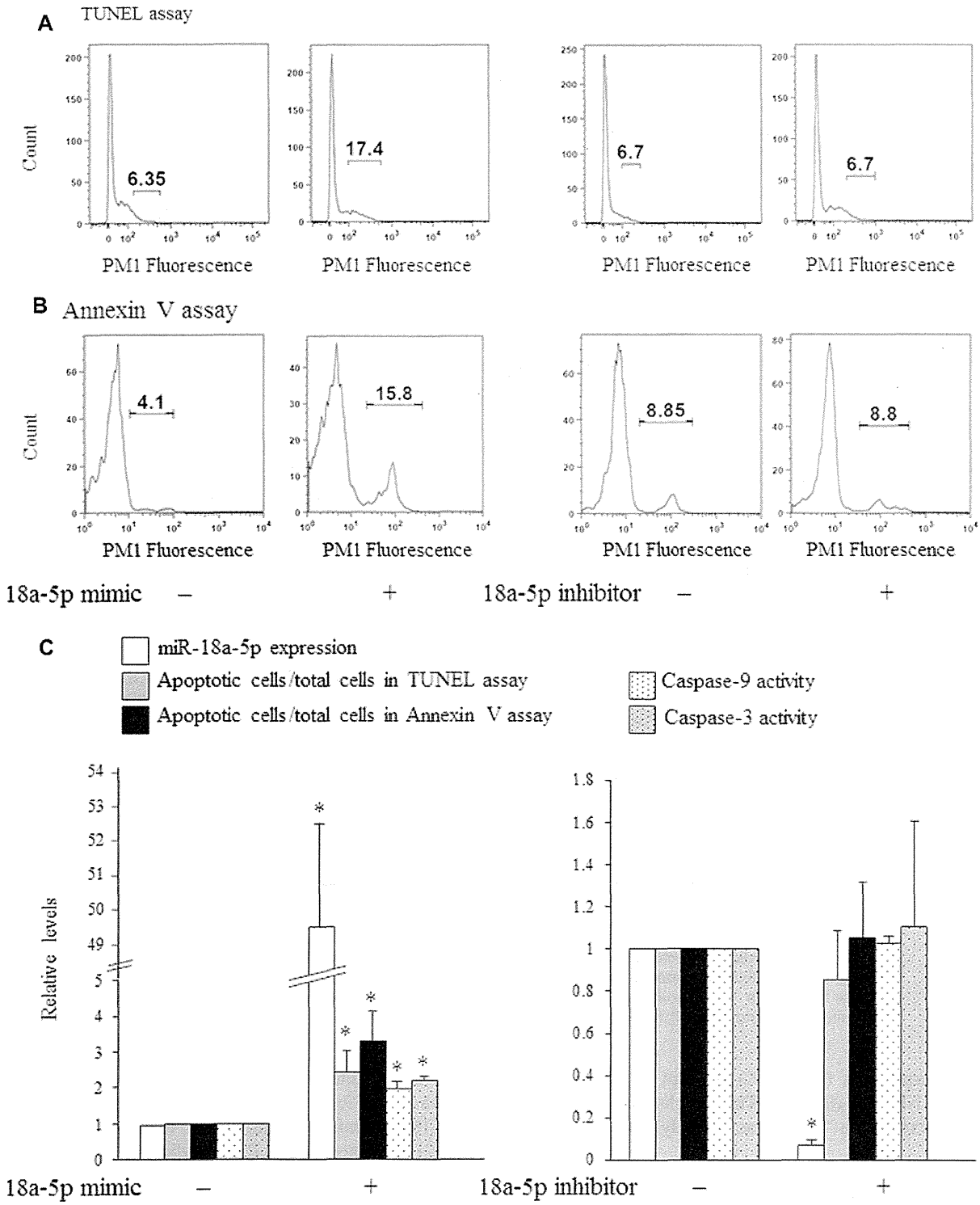

FIG 2. Role of miR-18a-5p in cell apoptosis. NHEKs were transfected with miR-18a-5p mimic, miR-18a-5p inhibitor, or controls for 72 hours. **A** and **B**, Flow cytometric histograms showing the percentage of apoptotic cells in the TUNEL or Annexin V assays. **C**, miR-18a-5p levels, relative apoptotic cell ratios by TUNEL or Annexin V assays, and activities of caspase-9 or caspase-3 (n = 3). **P* < .05 compared with control cells (1.0).

To investigate the relationship between miR-18a-5p and apoptosis, NHEKs were transfected with miR-18a-5p mimic, and the apoptosis of NHEKs was evaluated by using TUNEL (Fig 2, *A*) and Annexin V (Fig 2, *B*) assays. Overexpression of the miR-18a-5p mimic *in vitro* resulted in an increased percentage of apoptotic cells according to the 2 different apoptosis assays (Fig 2, *A* and *B*). The increase was statistically significant (Fig 2, *C*). On the other hand, miR-18a-5p inhibitor reduced

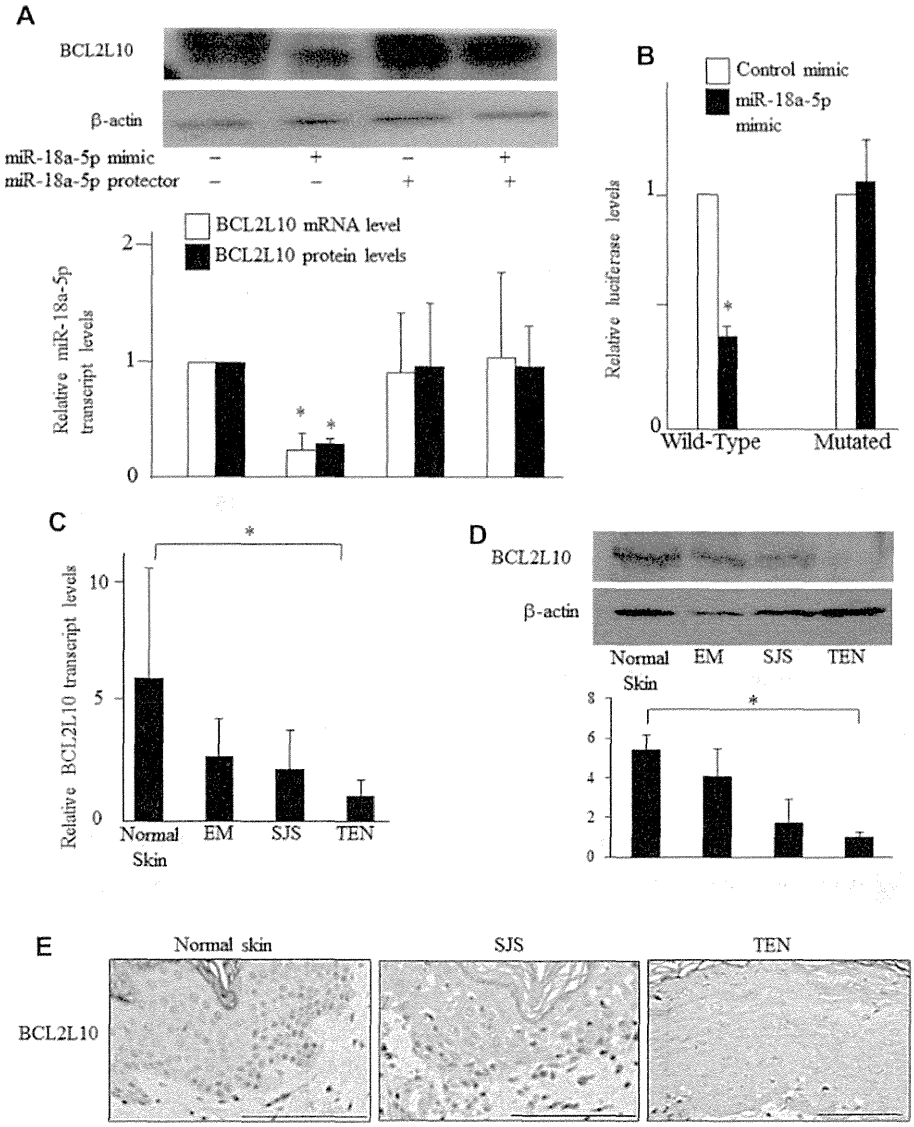

FIG 3. BCL2L10 expression *in vitro* and *in vivo*. **A,** BCL2L10 protein or mRNA levels in NHEKs transfected with miRNA mimics, protectors, or both (n = 3). **B,** NHEKs were transfected with wild-type or mutated BCL2L10 3′ UTR luciferase constructs together with control or miR-18a-5p mimic. The *bar graph* shows luciferase activities (n = 3). **C** and **D,** mRNA (Fig 3, *C*) or protein (Fig 3, *D*) levels of BCL2L10 in skin samples. **E,** Immunostaining of BCL2L10. *Bars* = 100 μm. *$P < .05$.

miR-18a-5p expression (Fig 2, *C*) but did not increase the apoptosis of NHEKs (Fig 2). This might be because the miR-18a-5p expression level was already low enough in NHEKs.

We searched for potential targets of miR-18a-5p by using the miRNA target gene prediction database. According to MicroCosm Targets (version 5, http://www.ebi.ac.uk/enright-srv/microcosm/htdocs/targets/v5/) and TargetScan (version 6.0, http://www.targetscan.org/), we focused on *BCL2L10*, a new member of the BCL-2 family, as an apoptosis-associated putative target gene of miR-18a-5p. To confirm the association between miR-18a-5p and *BCL2L10*, NHEKs were transfected with the miR-18a-5p mimic and/or the miScript Target Protector (Qiagen), single-stranded RNA complementary to the miR-18a-5p binding site on the *BCL2L10* mRNA 3′ UTR; the protector covers the flanking region of the binding site and specifically interferes with direct interaction between miRNA and mRNA.[25] As shown in Fig 3, *A*, in the presence of the control protector, the miR-18a-5p mimic significantly reduced the expression of BCL2L10 protein and mRNA, indicating *BCL2L10* is a target of miR-18a-5p. On the other hand, in the presence of the miR-18a-5p–specific protector, the suppressive effects of the miR-18a-5p mimic on BCL2L10 expression were attenuated. To further assess the direct binding of miR-18a-5p to the *BCL2L10* 3′ UTR, we performed a luciferase reporter gene assay using a luciferase construct containing wild-type *BCL2L10* 3′ UTR and that with point mutations, changing gcacctt into gcattcc to mutate the miR-18a-5p seed match.[26] The luciferase activity of the wild-type construct was reduced by the miR-18a-5p mimic, whereas that of the mutated construct was not (Fig 3, *B*). These results indicate that miR-18a-5p binds to the *BCL2L10* 3′ UTR and directly regulates BCL2L10 expression.

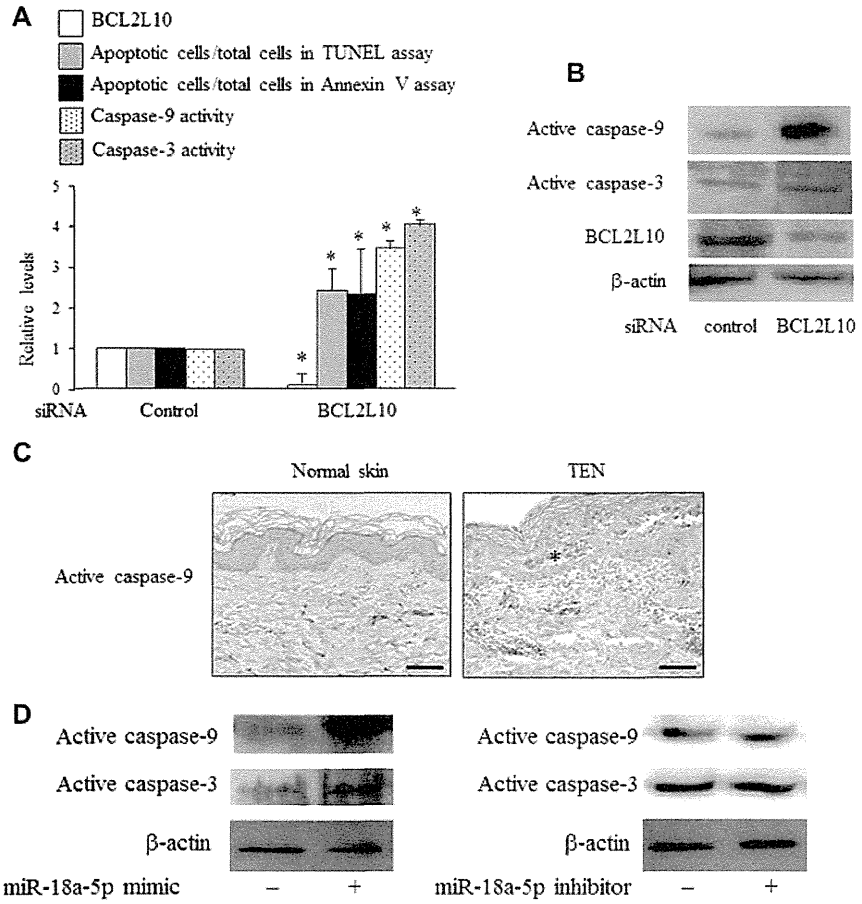

FIG 4. Function of BCL2L10 in patients with TEN. **A,** NHEKs were transfected with BCL2L10 siRNA for 72 hours. BCL2L10 mRNA levels, apoptotic cell ratios, and caspase activities are shown (n = 3). *$P < .05$. **B,** Immunoblotting with NHEKs transfected with BCL2L10 siRNA. **C,** Immunostaining of active caspase-9. *Bars* = 100 μm. *Asterisks* indicate apoptotic cells. **D,** NHEKs were transfected with miRNA mimics or inhibitors. Active caspases were determined by using immunoblotting.

Then we examined the expression levels of BCL2L10 in the skin tissues of patients with drug eruptions. There were significant decreases in the levels of *BCL2L10* mRNA (Fig 3, *C*) and protein (Fig 3, *D*) in the skin of patients with TEN compared with those seen in healthy skin. BCL2L10 levels were also decreased in patients with SJS and those with EM, although not significantly, indicating that the BCL2L10 expression tended to be inversely correlated with disease severity and the miR-18a-5p expression pattern, as shown in Fig 1, *A*.

Immunohistochemistry revealed that the protein expression of BCL2L10 was observed in the nuclei of keratinocytes in the normal epidermis, whereas its expression in the epidermis of patients with TEN was decreased (Fig 3, *E*). BCL2L10 expression was also reduced in patients with SJS slightly, which is consistent with the results shown in Fig 3, *C* and *D*.

The role of BCL2L10 in the skin has not yet been reported. When BCL2L10 expression was knocked down by siRNA (Fig 4, *A*), we observed a significant increase in apoptotic cell numbers using the TUNEL and Annexin V assays. Consistent with the notion that BCL2L10 is a member of the BCL-2 family and is known to inhibit the intrinsic apoptosis pathway (see Fig E1 in this article's Online Repository at www.jacionline.org), the protein expressions of active caspase-9, the key caspase of intrinsic apoptosis (Fig 4, *B*), and its activity (Fig 4, *A*) were also upregulated by the siRNA.

Taken together, our results showed that miR-18a-5p is overexpressed in the skin of patients with TEN, that miR-18a-5p is a suppressor of BCL2L10, and that BCL2L10 is a negative regulator of intrinsic keratinocyte apoptosis. We hypothesized that the downregulated BCL2L10 level caused by miR-18a-5p overexpression induces intrinsic apoptosis of keratinocytes in patients with TEN. Consistent with this hypothesis, caspase-9 was activated in the epidermis of patients with TEN compared with healthy skin (Fig 4, *C*). Of note, the apoptotic cells in the skin of patients with TEN strongly expressed active caspase-9. Furthermore, the miR-18a-5p mimic also induced the expression (Fig 4, *D*) and activity (Fig 2, *C*) of active caspase-9, as well as caspase-3, indicating that miR-18a-5p regulates intrinsic apoptosis. Consistent with the results of the apoptosis assay shown in Fig 2, miR-18a-5p inhibitor did not affect the expression or activity of caspases.

Serum levels of miR-18a-5p in patients with drug eruptions and their correlations with clinical features

We also compared the serum concentration of miR-18a-5p between patients with drug eruptions and healthy subjects. To

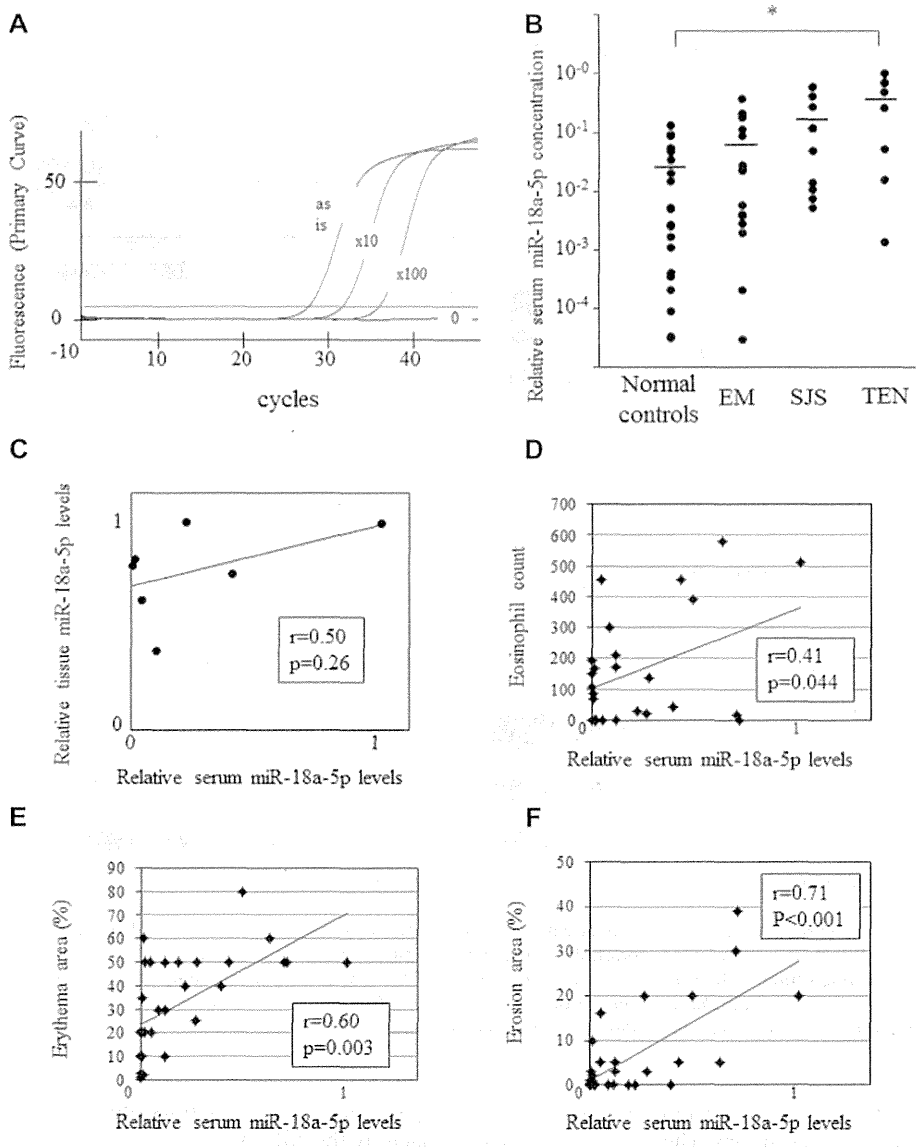

FIG 5. Serum concentrations of miR-18a-5p in patients with drug eruptions. **A,** Serial dilutions of cDNA (as is, 10-fold dilution, 100-fold dilution, and 0) synthesized from serum miRNA were used as templates for real-time PCR. **B,** Serum miR-18a-5p levels. *Bars* show means. *$P < .05$. **C,** Correlation between serum and skin miR-18-5p level of each patient. **D-F,** Correlation between serum miR-18a-5p levels and clinical features of patients.

validate that the miRNA is indeed detectable in human serum, miRNA was extracted from sera of healthy subjects, and the level of miR-18a-5p was determined by using real-time PCR with miR-18a-5p primer (Fig 5, *A*).[17-20] Amplification of miR-18a-5p was observed. The cycle threshold (Ct) value for miR-18a-5p in the undiluted miRNA sample was 27.8, and the values were increased by serial dilution of the template. Therefore miR-18a-5p is thought to be detectable and quantitative in the serum by using our method. We also verify the presence of miR-18-5p in human sera by sequencing the miR-18a-5p PCR product.

Serum miR-18a-5p levels were significantly increased in patients with TEN compared with those seen in healthy subjects, indicating they are useful for the diagnosis of TEN. Levels in patients with EM and those with SJS were slightly higher than those in healthy control subjects, although the differences were not statistically significant (Fig 5, *B*), which is consistent with the finding that the miR-18a-5p expression in the skin tended to be correlated with the severity of the drug eruption (Fig 1, *A*). Furthermore, as shown in Fig 5, *C*, we found a positive correlation ($r = 0.50$) between the serum miR-18a-5p level and miR-18a-5p expression in the skin tissue of each patient, although it was not statistically significant.

Therefore we next analyzed the associations between serum miR-18a-5p levels and the clinical features of drug eruptions. Serum miR-18a-5p levels exhibited a poor correlation with eosinophil counts ($r = 0.48$, $P = .010$; Fig 5, *D*). On the other hand, serum miR-18a-5p levels were correlated with the BSA of erythema ($r = 0.60$, $P = .003$; Fig 5, *E*) and the BSA of erosion ($r = 0.71$, $P < .001$; Fig 5, *F*) more strongly. Taken together, the serum level of miR-18a-5p can also be used as a disease activity marker for drug eruptions, reflecting the severity of keratinocyte apoptosis.

DISCUSSION

This study demonstrated the role of the miR-18a-5p–BCL2L10 pathway in keratinocyte apoptosis and its contribution to the pathogenesis of TEN based on 3 major findings.

First, we found that the upregulation of miR-18a-5p can be highly specific to TEN. In addition, the miR-18a-5p expression was correlated with the severity of drug eruptions. According to recent reports, miR-18a-5p is involved in the pathogenesis of basal cell carcinoma, ataxia-telangiectasia, and pancreatic cancer.[27-29] This is the first study to investigate miR-18a-5p expression in patients with allergic skin diseases. According to the array, miR-18a-5p and miR-18b-5p exhibited different expression patterns in various skin diseases. miR-18a-5p and miR-18b-5p have a similar sequence; however, their source is chromosome 13 and chromosome X, respectively. Therefore they are likely regulated independently. The regulatory mechanism of miR-18a-5p overexpression in patients with TEN remains unclear. miRNA expression can be regulated by various stimuli, including activation of transcription factors and methylation in general. However, investigation of abnormalities in these factors in patients with TEN has just begun. Further studies are needed to clarify the mechanism.

miR-18a-5p overexpression resulted in an increase in cell apoptosis. miR-17-3p and miR-92a-3p, other members of the miR-17-92 cluster, are reported to be more important for the regulation of apoptosis in thyroid cancer cells or colon cancer cells than miR-18a-5p.[30,31] However, their expression was not significantly increased in the skin of patients with TEN in our study. Our results suggest that miR-18a-5p is also involved in the apoptosis pathway and that its effects on apoptosis might be cell type dependent.

Second, we also found new miRNA-mRNA target interactions in this study; upregulated miR-18a-5p led to decreased expression of BCL2L10 in keratinocytes. Immunohistochemical staining showed that BCL2L10 proteins were expressed in the epidermal layers of healthy skin. In addition, *BCL2L10* siRNA and miR-18a-5p mimic upregulated keratinocyte apoptosis, indicating that BCL2L10 acts as an antiapoptotic regulator in the skin. There are several reports about the relationships between BCL2L10 and gastric cancer, breast cancer, and leukemia.[32-34] However, the role of BCL2L10 in skin diseases remains unknown. This study is the first to clarify the function and localization of BCL2L10 in the skin. BCL2L10 is one of the 6 antiapoptotic members of the BCL-2 family, the key regulators of apoptosis,[35] and is involved in the intrinsic apoptosis pathway. There are both extrinsic and intrinsic pathways in apoptosis (see Fig E1). The extrinsic pathway is activated by the binding of Fas ligand or TNF to the death receptor. The receptor contains an intracellular death domain and activates caspase-8 and subsequently caspase-3. On the other hand, in the intrinsic pathway proapoptotic proteins (BAX and BAK) cause mitochondrial outer membrane permeabilization, resulting in the release of cytochrome C. This stimulates the activation of caspase-9 and caspase-3 and then induces cell death.[36] The antiapoptotic members of the BCL-2 family (BCL2, BCL2L1, BCL2L2, BCL2A1, MCL1, and BCL2L10) inhibit the activity of BAX or BAK to lead cells toward survival.[37-39] According to previous reports, extrinsic pathways, such as Fas, are implicated in the mechanisms underlying the apoptosis observed in patients with TEN.[1,2] The present study demonstrated caspase-9 activation in the epidermis of patients with TEN and suggested that the intrinsic pathway is also activated. The miR-18a-5p-BCL2L10 pathway might contribute to this process.

The inhibition of endogenous miR-18a-5p expression in NHEKs did not influence apoptosis and expression of BCL2L10. Thus we could not show the therapeutic potential of miR-18a-5p inhibitors for the treatment of TEN. To further evaluate therapeutic values, miR-18a-5p inhibition needs to be tested by using an *in vitro* or *in vivo* model of TEN. Widely accepted models should to be developed in the future.

Lastly, we first investigated serum miRNA levels in patients with drug eruptions. There is only 1 report showing that miR-18a-5p is detectable and quantitative in body fluid. In that study miR-18a-5p was found to be increased in the plasma of patients with pancreatic cancer.[28] Our results indicate that serum miR-18a-5p concentrations were significantly increased in patients with TEN and correlated with the severity of drug eruptions, which is consistent with the expression pattern of miR-18a-5p in the skin. We often experience patients with TEN whose diagnoses are incorrect and who are not treated intensively in the early stage, which results in permanent damage to the eyes or esophagus and even death. Therefore it is urgent to develop reliable diagnostic markers and disease activity markers for TEN. Soluble Fas ligand has become such a candidate diagnostic marker, and recently, Fujita et al[40] had a rapid immunochromatographic assay for the detection of increased serum levels of granulysin, a cytolytic proapoptotic protein, found in patients with TEN. Our study suggests that the serum miR-18a-5p level might also be a useful disease marker. Although we did not find any differences in miR-18a levels between patients induced by different drugs, this might be due to the small number of patients. Larger studies are needed to evaluate the future clinical use of this marker.

In summary, miR-18a-5p can play a key role in the keratinocyte apoptosis observed in patients with drug eruptions, especially in patients with TEN. Investigating the regulatory mechanisms of keratinocyte apoptosis induced by miRNAs might lead to the development of new disease markers.

We thank Ms Tomomi Kira and Ms Chiemi Shiotsu for their valuable technical assistance.

Key messages

- miR-18a-5p expression is upregulated in the skin of patients with TEN.
- Increased miR-18a-5p expression and subsequently decreased BCL2L10 expression might play key roles in the intrinsic keratinocyte apoptosis observed in patients with TEN.
- Serum miR-18a-5p levels are significantly increased in patients with TEN.

REFERENCES

1. Abe R, Shimizu T, Shibaki A, Nakamura H, Watanabe H, Shimizu H. Toxic epidermal necrolysis and Stevens-Johnson syndrome are induced by soluble Fas ligand. Am J Pathol 2003;162:1515-20.
2. Chung WH, Hung SI, Yang JY, Su SC, Huang SP, Wei CY, et al. Granulysin is a key mediator for disseminated keratinocyte death in Stevens-Johnson syndrome and toxic epidermal necrolysis. Nat Med 2008;14:1343-50.

3. Sand M, Gambichler T, Sand D, Skrygan M, Altmeyer P, Bechara F. MicroRNAs and the skin: tiny players in the body's largest organ. J Dermatol Sci 2009;53:169-75.
4. Filipowicz W, Jaskiewicz L, Kolb FA, Pillai RS. Post-transcriptional gene silencing by siRNAs and miRNAs. Curr Opin Struct Biol 2005;15:331-41.
5. Bartel D. MicroRNAs: genomics, biogenesis, mechanism, and function. Cell 2004;116:281-97.
6. Friedman R, Farh K, Burge C, Bartel D. Most mammalian mRNAs are conserved targets of microRNAs. Genome Res 2009;19:92-105.
7. Bostjancic E, Glavac D. Importance of microRNAs in skin morphogenesis and diseases. Acta Dermatovenerol Alp Panonica Adriat 2008;17:95-102.
8. Herrera B, Lockstone H, Taylor J, Ria M, Barrett A, Collins S, et al. Global microRNA expression profiles in insulin target tissues in a spontaneous rat model of type 2 diabetes. Diabetologia 2010;53:1099-109.
9. Chen Y, Gorski D. Regulation of angiogenesis through a microRNA (miR-130a) that down-regulates antiangiogenic homeobox genes GAX and HOXA5. Blood 2008;111:1217-26.
10. Davidson-Moncada J, Papavasiliou F, Tam W. MicroRNAs of the immune system: roles in inflammation and cancer. Ann N Y Acad Sci 2010;1183:183-94.
11. Kuehbacher A, Urbich C, Dimmeler S. Targeting microRNA expression to regulate angiogenesis. Trends Pharmacol Sci 2008;29:12-5.
12. Furer V, Greenberg J, Attur M, Abramson S, Pillinger M. The role of microRNA in rheumatoid arthritis and other autoimmune diseases. Clin Immunol 2010;136:1-15.
13. Cheng Y, Zhang C. MicroRNA-21 in cardiovascular disease. J Cardiovasc Transl Res 2010;3:251-5.
14. Provost P. MicroRNAs as a molecular basis for mental retardation, Alzheimer's and prion diseases. Brain Res 2010;1338:58-66.
15. Wei CY, Ko TM, Shen CY, Chen YT. A recent update of pharmacogenomics in drug-induced severe skin reactions. Drug Metab Pharmacokinet 2012;27:132-41.
16. Nakashima T, Jinnin M, Etoh T, Fukushima S, Masuguchi S, Maruo K, et al. Down-regulation of mir-424 contributes to the abnormal angiogenesis via MEK1 and cyclin E1 in senile hemangioma: its implications to therapy. PLoS One 2010;5:e14334.
17. Kroh E, Parkin R, Mitchell P, Tewari M. Analysis of circulating microRNA biomarkers in plasma and serum using quantitative reverse transcription-PCR (qRT-PCR). Methods 2010;50:298-301.
18. Mitchell PS, Parkin RK, Kroh EM, Fritz BR, Wyman SK, Pogosova-Agadjanyan EL, et al. Circulating microRNAs as stable blood-based markers for cancer detection. Proc Natl Acad Sci U S A 2008;105:10513-8.
19. Gilad S, Meiri E, Yogev Y, Benjamin S, Lebanony D, Yerushalmi N, et al. Serum microRNAs are promising novel biomarkers. PLoS One 2008;3:e3148.
20. Zhu W, Qin W, Atasoy U, Sauter ER. Circulating microRNAs in breast cancer and healthy subjects. BMC Res Notes 2009;2:89.
21. Kanemaru H, Fukushima S, Yamashita J, Honda N, Oyama R, Kakimoto A, et al. The circulating microRNA-221 level in patients with malignant melanoma as a new tumor marker. J Dermatol Sci 2011;61:187-93.
22. Jimeno A, Rubio-Viqueira B, Amador ML, Oppenheimer D, Bouraoud N, Kulesza P, et al. Epidermal growth factor receptor dynamics influences response to epidermal growth factor receptor targeted agents. Cancer Res 2005;65:3003-10.
23. Lu Z, Ding L, Hong H, Hoggard J, Lu Q, Chen YH. Claudin-7 inhibits human lung cancer cell migration and invasion through ERK/MAPK signaling pathway. Exp Cell Res 2011;317:1935-46.
24. Storey JD, Tibshirani R. Statistical significance for genomewide studies. Proc Natl Acad Sci U S A 2003;100:9440-5.
25. Long JM, Lahiri DK. MicroRNA-101 downregulates Alzheimer's amyloid-β precursor protein levels in human cell cultures and is differentially expressed. Biochem Biophys Res Commun 2011;404:889-95.
26. Brock M, Trenkmann M, Gay RE, Gay S, Speich R, Huber LC. MicroRNA-18a enhances the interleukin-6-mediated production of the acute-phase proteins fibrinogen and haptoglobin in human hepatocytes. J Biol Chem 2011;286:40142-50.
27. Sand M, Skrygan M, Sand D, Georgas D, Hahn S, Gambichler T, et al. Expression of microRNAs in basal cell carcinoma. Br J Dermatol 2012;167:847-55.
28. Morimura R, Komatsu S, Ichikawa D, Takeshita H, Tsujiura M, Nagata H, et al. Novel diagnostic value of circulating miR-18a in plasma of patients with pancreatic cancer. Br J Cancer 2011;105:1733-40.
29. Song L, Lin C, Wu Z, Gong H, Zeng Y, Wu J, et al. miR-18a impairs DNA damage response through downregulation of ataxia telangiectasia mutated (ATM) kinase. PLoS One 2011;6:e25454.
30. Takakura S, Mitsutake N, Nakashima M, Namba H, Saenko VA, Rogounovitch TI, et al. Oncogenic role of miR-17-92 cluster in anaplastic thyroid cancer cells. Cancer Sci 2008;99:1147-54.
31. Tsuchida A, Ohno S, Wu W, Borjigin N, Fujita K, Aoki T, et al. miR-92 is a key oncogenic component of the miR-17-92 cluster in colon cancer. Cancer Sci 2011;102:2264-71.
32. Xu JD, Cao XX, Long ZW, Liu XP, Furuya T, Xu JW, et al. BCL2L10 protein regulates apoptosis/proliferation through differential pathways in gastric cancer cells. J Pathol 2011;223:400-9.
33. Tvrdík D, Skálová H, Dundr P, Povýšil C, Velenská Z, Berková A, et al. Apoptosis-associated genes and their role in predicting responses to neoadjuvant breast cancer treatment. Med Sci Monit 2012;18:BR60-7.
34. Voso MT, Fabiani E, Piciocchi A, Matteucci C, Brandimarte L, Finelli C, et al. Role of BCL2L10 methylation and TET2 mutations in higher risk myelodysplastic syndromes treated with 5-azacytidine. Leukemia 2011;25:1910-3.
35. Lanave C, Santamaria M, Saccone C. Comparative genomics: the evolutionary history of the Bcl-2 family. Gene 2004;333:71-9.
36. Youle RJ, Strasser A. The BCL-2 protein family: opposing activities that mediate cell death. Nat Rev Mol Cell Biol 2008;9:47-59.
37. Edlich F, Banerjee S, Suzuki M, Cleland MM, Arnoult D, Wang C, et al. Bcl-x(L) retrotranslocates Bax from the mitochondria into the cytosol. Cell 2011;145:104-16.
38. Willis SN, Fletcher JI, Kaufmann T, van Delft MF, Chen L, Czabotar PE, et al. Apoptosis initiated when BH3 ligands engage multiple Bcl-2 homologs, not Bax or Bak. Science 2007;315:856-9.
39. Chipuk JE, Moldoveanu T, Llambi F, Parsons MJ, Green DR. The BCL-2 family reunion. Mol Cell 2010;37:299-310.
40. Fujita Y, Yoshioka N, Abe R, Murata J, Hoshina D, Mae H, et al. Rapid immunochromatographic test for serum granulysin is useful for the prediction of Stevens-Johnson syndrome and toxic epidermal necrolysis. J Am Acad Dermatol 2011;65:65-8.

Letter to the Editor

Analysis of expression pattern of serum microRNA levels in patients with psoriasis

Keywords:
Inflammatory skin diseases; Epigenetics; microRNA

Psoriasis vulgaris (PV) is sometimes difficult to be distinguished from eczemas, lymphomas, drug eruptions or syphilis. Thus, reliable serum markers of PV are needed. We determined serum levels of 6 microRNAs (miRNAs) in individual patient by real-time PCR as described previously [1,2], and tried to differentiate PV patients from normal subjects or patients with other diseases by combination of miRNA levels. The 6 miRNAs were selected because they are reported to be involved in the pathogenesis of PV at least in two different previous studies [3–10]. The detailed methodologies are described in Supplementary data.

First, serum levels of the 6 miRNAs were measured in 15 normal subjects, 15 atopic dermatitis (AD) patients and 15 PV patients (Tables S1 and S2). We found statistically significant difference in the levels of miR-125b, miR-146a, miR-203 and miR-205 among normal subjects, AD patients and PV patients using Kruskal–Wallis test ($P = 0.0076$, 0.00064, 0.00002 and 0.011, respectively). Serum levels of miR-125b, miR-146a, miR-203 and miR-205 were significantly decreased in PV patients compared with normal subjects ($P = 0.017$, 0.00042, 0.000075 and 0.0066, respectively) by Mann–Whitney test (Fig. 1), whereas significant difference was seen only in miR-125b levels between normal subjects and AD patients ($P = 0.0032$). When receiver operating characteristics (ROC) curves of all 6 miRNA levels were analyzed, the serum levels of miR-203, miRNA which is most significantly down-regulated in PV patients as described above, might serve as more useful biomarker for differentiating PV patients and normal subjects with the areas under curves (AUCs) of 0.92 than levels of other 5 miRNAs (Fig. S1): according to the Youden index, the most optical cut-off point was set at 0.31 (sensitivity 87%, specificity 93%, Youden index 0.8). Furthermore, among all the possible combinations, the combination of miR-146a and -203 levels was the best to improve the AUC (0.94), although the sensitivity (87%) and specificity (93%) at the most optical cut-off point (0.94) remained the same (Youden index 0.8). On the other hand, AUC was 0.58 by miR-203 alone and 0.52 by miR-146a and miR-203 for differentiating normal subjects and AD patients. Thus, the combination of miR-146a and -203 levels may be useful for the diagnosis of PV, but not for AD.

To prove our hypothesis that the combination of miR-146a and -203 levels shows higher AUC than level of each miRNA for the diagnosis of PV, we validated it in a new data set including 10 PV patients, 9 normal subjects and 7 patients with cutaneous lymphoma, another differential diagnosis (Fig. 2, Tables S3 and S4). As shown in Fig. S2, miR-203 levels had the AUC 0.89 to distinguish normal subjects from PV patients, whereas the combination of miR-146 and -203 levels improved the AUC (0.94). Similarly, the AUC of miR-203 levels to distinguish PV patients from lymphoma patients was 0.84, while the AUC was increased (0.86) by the combination with miR-146a levels. Thus, the combination of miRNA levels may be more reliable to distinguish PV patients from normal subjects or patients with differential diagnosis than level of each miRNA alone.

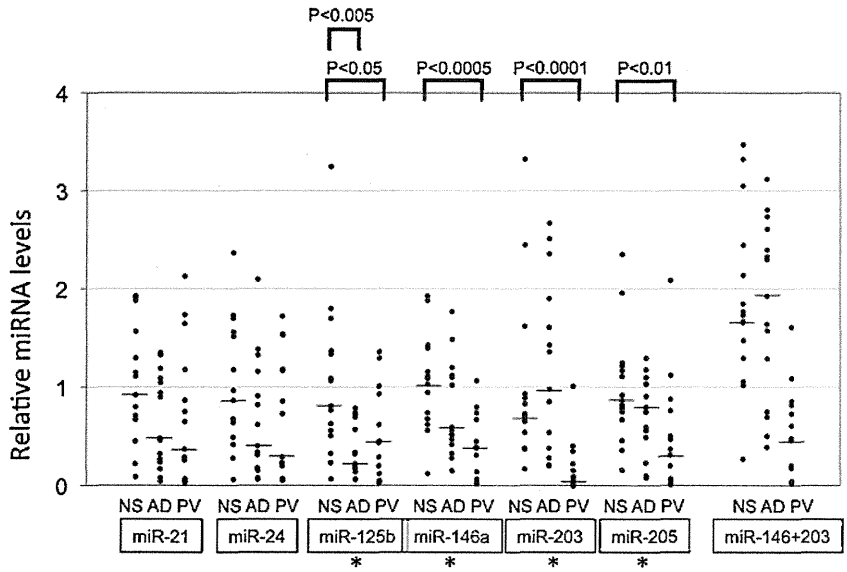

Fig. 1. Relative miRNA concentrations determined by real-time PCR as described in Table S1 are shown on the ordinate. Bars show medians. *Indicates $P \leq 0.05$ among normal subjects (NS), atopic dermatitis (AD) and psoriasis vulgaris (PV) in each miRNA level by Kruskal–Wallis test. *P* values above the bar graphs were calculated by Mann–Whitney test.

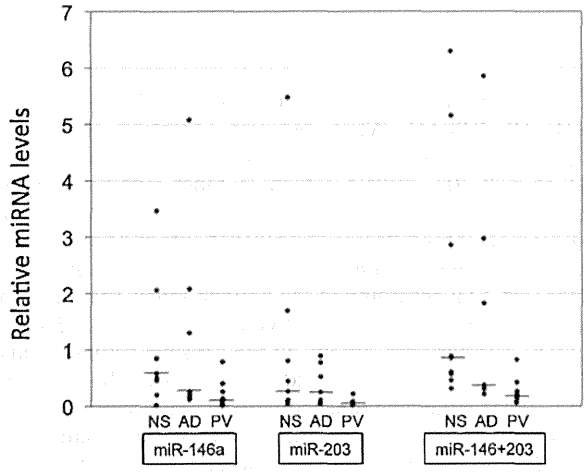

Fig. 2. Relative miRNA concentrations determined by real-time PCR as described in Table S3 are shown on the ordinate.

Acknowledgements

This study was supported in part by a grant for scientific research from the Japanese Ministry of Education, Science, Sports and Culture, by Shiseido Research Grant, and by grants from Rohto Award.

Appendix A. Supplementary data

Supplementary material related to this article can be found, in the online version, at http://dx.doi.org/10.1016/j.jdermsci. 2014.01. 005.

References

[1] Kroh EM, Parkin RK, Mitchell PS, Tewari M. Analysis of circulating microRNA biomarkers in plasma and serum using quantitative reverse transcription-PCR (qRT-PCR). Methods 2010;50(4):298–301.

[2] Kanemaru H, Fukushima S, Yamashita J, Honda N, Oyama R, Kakimoto A, et al. The circulating microRNA-221 level in patients with malignant melanoma as a new tumor marker. J Dermatol Sci 2011;61(3):187–93.

[3] Sonkoly E, Wei T, Janson PC, Sääf A, Lundeberg L, Tengvall-Linder M, et al. microRNAs: novel regulators involved in the pathogenesis of psoriasis? PLoS One 2007;2(7):e610.

[4] Sonkoly E, Ståhle M, Pivarcsi A. microRNAs: novel regulators in skin inflammation. Clin Exp Dermatol 2008;33(3):312–5.

[5] Zibert JR, Løvendorf MB, Litman T, Olsen J, Kaczkowski B, Skov L. microRNAs and potential target interactions in psoriasis. J Dermatol Sci 2010;58(3): 177–85.

[6] Joyce CE, Zhou X, Xia J, Ryan C, Thrash B, Menter A, et al. Deep sequencing of small RNAs from human skin reveals major alterations in the psoriasis miRNAome. Hum Mol Genet 2011;20(20):4025–40.

[7] Xu N, Brodin P, Wei T, Meisgen F, Eidsmo L, Nagy N, et al. MiR-125b: a microRNA downregulated in psoriasis, modulates keratinocyte proliferation by targeting FGFR2. J Invest Dermatol 2011;131(7):1521–9.

[8] Gu X, Nylander E, Coates PJ, Nylander K. Effect of narrow-band ultraviolet B phototherapy on p63 and microRNA (miR-21 and miR-125b) expression in psoriatic epidermis. Acta Derm Venereol 2011;91(4):392–7.

[9] Ralfkiaer U, Hagedorn PH, Bangsgaard N, Løvendorf MB, Ahler CB, Svensson L, et al. Diagnostic microRNA profiling in cutaneous T-cell lymphoma (CTCL). Blood 2011;118(22):5891–900.

[10] Bhandari A, Gordon W, Dizon D, Hopkin AS, Gordon E, Yu Z, Andersen B. The Grainyhead transcription factor Grhl3/Get1 suppresses miR-21 expression and tumorigenesis in skin: modulation of the miR-21 target MSH2 by RNA-binding protein DND1. Oncogene 2012;32(12):1497–507.

Yusaku Koga, Masatoshi Jinnin*, Asako Ichihara, Akihiko Fujisawa, Chikako Moriya, Keisuke Sakai, Satoshi Fukushima, Yuji Inoue, Hironobu Ihn

Department of Dermatology and Plastic Surgery, Faculty of Life Sciences, Kumamoto University, 1-1-1 Honjo, Kumamoto 860-8556, Japan

*Corresponding author. Tel.: +81 96 373 5233; fax: +81 96 373 5235

E-mail addresses: mjin@kumamoto-u.ac.jp, jinjin1011@hotmail.com (M. Jinnin).

Received 28 July 2013

http://dx.doi.org/10.1016/j.jdermsci.2014.01.005

Photodynamic diagnosis of metastatic lymph nodes using 5-aminolevulinic acid in mouse squamous cell carcinoma

Keywords:
Squamous cell carcinoma; Photodynamic diagnosis; 5-Aminolevulinic acid; Protoporphyrin IX

To the Editor

Squamous cell carcinoma (SCCs) is one of the most frequent types of non-melanoma skin cancer. In certain cases, SCCs spread to the regional lymph nodes (LNs), which results in poor prognosis. It is essential to accurately evaluate LN metastasis in order to select the appropriate therapeutic strategy and predict the outcomes of the patients with SCCs. In addition to using sentinel lymph node biopsy (SLNB), which is a potentially promising procedure for assessing LN metastasis in patients with SCCs [1], achieving accurate and rapid intraoperative diagnosis is vital to ensure the use of a less invasive surgery.

The photosensitizer 5-aminolevulinic acid (5-ALA) has recently been clinically used for detecting the primary lesion in certain types of non-melanoma skin cancers—this process is termed as photodynamic diagnosis. The exogenous administration of 5-ALA causes selective accumulation of the heme precursor protoporphyrin IX (PpIX) in cancer cells [2]. PpIX is a fluorescent substance that emits a strong red fluorescence at approximately 635 nm on blue light excitation [3,4].

In the present study, we aimed to evaluate the feasibility of using 5-ALA-induced PpIX fluorescence as a rapid intraoperative diagnostic tool for LN metastasis in mouse SCCs.

A mouse model of SCCs with LN metastasis was established, as previously described by Matsumoto et al. [5] with minor modifications. In brief, NR-S1M cells (6×10^6 cells) were intracutaneously injected into the back area—adjacent to the tail—of 6–8-week-old C3H/He mice (SHIMIZU Laboratory Supplies, Kyoto, Japan). Three to four weeks after tumor implantation, the mice were administered 5-ALA hydrochloride (Wako Pure Chemical Industries, Kyoto, Japan) at a dose of 250 mg/kg body weight through a tail vein injection [6]. Six to nine hours after the injection, the inguinal, axiliary, and para-aortic LNs were excised and examined using fluorescence stereomicroscopy, as described previously [6,7]. Briefly, light emitting from a mercury lamp was filtered through a 405 ± 10 nm band-pass filter and used for excitation. The fluorescent emission at a wavelength longer than 430 nm was transmitted through a long-pass filter and detected by charge-coupled device camera. We performed intensity analysis by

Arch Dermatol Res (2014) 306:367–374
DOI 10.1007/s00403-014-1452-z

ORIGINAL PAPER

miR-205 down-regulation promotes proliferation of dermatofibrosarcoma protuberans tumor cells by regulating LRP-1 and ERK phosphorylation

Ikko Kajihara · Masatoshi Jinnin · Miho Harada · Katsunari Makino · Noritoshi Honda · Takamitsu Makino · Toshikatsu Igata · Shinichi Masuguchi · Satoshi Fukushima · Hironobu Ihn

Received: 5 July 2013 / Revised: 10 January 2014 / Accepted: 28 January 2014 / Published online: 14 February 2014

Abstract Dermatofibrosarcoma protuberans (DFSP) is an intermediate malignancy of the skin. Although COL1A1/PDGFB fusion gene was identified in the tumor cells recently, not all of the cases were positive for the fusion gene, and further researches are still needed to clarify the pathogenesis of DFSP. In this study, we investigated the role of microRNAs in the tumor. microRNA PCR array showed several microRNAs increased or decreased in DFSP in vivo compared with dermatofibroma (DF) and normal skin. Among them, the expression of miR-205 was down-regulated in DFSP compared with DF and normal skin. In situ hybridization showed that miR-205 expression was evident in dermal fibroblasts of normal skin although hardly detected in tumor cells of DF or DFSP. miR-205 inhibitor increased cell proliferation and the luciferase activity of 3′UTR of low-density lipoprotein receptor-related protein-1 (LRP-1) in cultured normal dermal fibroblasts. Immunohistochemistry showed the expression of LRP-1 was increased in DFSP tissue. Knockdown of LRP-1 suppressed cell growth and down-regulated extracellular signal-regulated kinase (ERK) phosphorylation without affecting MEK phosphorylation in cultured DFSP cells. Taken together, LRP-1 overexpression caused by the miR-205 down-regulation may play a role in the abnormal proliferation of DFSP cells via directly regulating ERK phosphorylation.

I. Kajihara · M. Jinnin (✉) · M. Harada · K. Makino · N. Honda · T. Makino · T. Igata · S. Masuguchi · S. Fukushima · H. Ihn
Department of Dermatology and Plastic Surgery, Faculty of Life Sciences, Kumamoto University, 1-1-1 Honjo, Kumamoto, Japan
e-mail: jinjin1011@hotmail.com

Keywords microRNA · Malignant soft tissue tumor · Fibroblast

Introduction

DFSP is a dermal neoplasm of intermediate malignancy, which is slow-growing with rare metastasis but locally invasive. Immunohistochemical analysis and electron microscopic studies have suggested that DFSP is of fibroblastic origin [1, 9]. Most of tumor cells of DFSP are positive for CD34 and negative for factor XIIIa. Furthermore, recently chimeric COL1A1/PDGFB transcript was identified [24, 26, 29]. Several reports indicated the COL1A1–PDGFB protein encoded by the fusion gene perhaps activates PDGF receptor β, which induces the abnormal proliferation of tumor cells [10, 28, 31]. Nevertheless, some cases were not positive for the fusion gene [30]. In addition, although imatinib mesylate, inhibitor of PDGF receptor β, was expected to have therapeutic value, phase II clinical trials did not show reasonable efficacy [17, 27]. Accordingly, further researches are still needed to clarify the pathogenesis of DFSP.

In vitro, cultured DFSP tumor cells show increased phosphorylation of ERK compared with normal dermal fibroblasts [13]. Moreover, the dysregulation of thrombospondin-1 is also reported in DFSP [21] However, little is known about the trigger of the oncogenesis of DFSP.

Recently, microRNAs (miRNAs) have attracted attention for their involvement in the etiology of various diseases including cancers, autoimmune diseases and inflammatory diseases [4, 12, 16]. miRNAs are short ribonucleic acid molecules (only 22 nucleotides long, on average) acting as post-transcriptional regulators that bind to complementary sequences in the 3′ untranslated regions

(3′ UTRs) of target mRNAs and subsequently leading to gene silencing [3, 6]. However, the role of miRNAs in DFSP is not examined.

In the current study, we tried to evaluate the possibility that miRNAs may play some roles in the pathogenesis of DFSP.

Materials and methods

Patient materials

Skin samples were obtained from tumor tissues of DFSP and DF. Control skin samples were obtained from routinely discarded skin of healthy subjects undergoing skin graft. Institutional review board approval and written informed consent were obtained before patients and healthy volunteers were entered into this study according to the Declaration of Helsinki. Immediately after removal, skin samples were fixed by formalin and embedded in paraffin.

Cell culture

The cultured DFSP tumor cells and normal dermal fibroblasts were obtained as described previously [13]. Primary explant cultures were established in 25-cm^2 culture flasks in modified Eagle's medium (MEM) supplemented with 10 % fetal calf serum (FCS) and Antibiotic–Antimycotic (Invitrogen, Carlsbad, CA). Monolayer cultures independently isolated from different individuals were maintained at 37 °C in 5 % CO_2. Before experiments, cells were serum-starved for 24 h.

Cell lysis and immunoblotting

Fibroblasts were cultured until they were confluent, and then cells were harvested. Cell lysates (normalized for protein concentration) were analyzed by immunoblotting as described previously [22]. Antibodies for phospho-p44/42 MAPK, p44/42 MAPK, MEK 1/2 and phospho-MEK 1/2 were purchased from Cell Signaling technology (Beverly, MA). Antibodies against β-actin and LRP-1 were obtained from Santa Cruz Biotechnology (Santa Cruz, CA) and R and D Systems (Minneapolis, MN), respectively.

Immunohistochemistry

Wax-embedded sections were dewaxed in xylene and rehydrated in graded alcohols. Antigens were retrieved by incubation with antigen retrieval solution (pH9, Nichirei, Tokyo, Japan) for 10 min at 121 °C. Immunohistochemistry was performed with the LRP-1 antibody (1:50) as described previously [15].

miRNA isolation and PCR array

miRNAs were extracted from paraffin sections of skin samples using miRNeasy FFPE kit (Qiagen, Valencia, CA). For miRNA PCR array, miRNAs were reverse-transcribed into first strand cDNA using RT2 miRNA First Strand Kit (SABiosciences, Frederick, MD). The cDNA was mixed with RT2 SYBR Green/ROX qPCR Master Mix, and the mixture was added into 96-well RT2 Human Cancer miRNA PCR Array (MAH-102A, SABioscience). PCR was performed on Takara Thermal Cycler Dice instrument (TP800®, Shiga, Japan). The raw Ct of each miRNA was normalized using U6.

Cell count

Cell counting was performed with Coulter Particle Counter as described previously [15].

In situ hybridization

In situ hybridization was performed with 5′-locked digoxigenin-labeled nucleic acid (LNA) probes complementary to human mature miR-205 or U6 positive control (Exiqon, Vedbeak, Denmark) [23, 25]. Briefly, sections were deparaffinized and deproteinized with protease K (Wako, Osaka, Japan) for 5 min. Slides were washed in 0.2 % glycine in PBS and fixed with 4 % paraformaldehyde. Hybridization was performed at 55 °C for 24 h. The sections were blocked with 2 % fetal bovine serum and 2 % bovine serum albumin in PBS and 0.1 % Tween 20 (PBST) for 1 h. The probe-target complex was detected immunologically by digoxigenin antibody conjugated to alkaline phosphatase acting on the chromogen nitro blue tetrazolium/5-bromo-4-chloro-3-indolyl phosphate (Roche Applied Science, Mannheim, Germany). The slides were counterstained with nuclear fast red, and examined under a light microscope (OLYMPUS BX50, Tokyo, Japan).

Transient transfection

miRNA inhibitors and mimics were purchased from Qiagen. Lipofectamine RNAiMAX (Invitrogen, Carlsbad, CA) was used as a transfection reagent. For reverse transfection, miRNA inhibitors (50 nmol/L, Qiagen) and mimics (5 nmol/L) mixed with transfection reagent were added when cells were plated, followed by incubation for 72 h at 37 °C in 5 % CO_2-enriched air. Control experiments showed transcript levels for target of miRNA inhibitors to be reduced by >80 %, and expression of miRNAs was increased at least fivefold by the transfection of mimics (data not shown).

LRP-1 siRNA and negative control siRNA was purchased from Dharmacon (Rockford, IL). The cells were transfected with siRNAs mixed with lipofectamine (Invitrogen) as a transfection reagent, and incubated for 96 h at 37 °C in 5 % CO_2.

Luciferase reporter assay

A luciferase reporter plasmid containing the LRP-1 3′UTR was purchased from GeneCopoeia (Rockville, MD). miRNA inhibitors (50 nmol/L) and reporter plasmid (Invitrogen, Carlsbad, CA) mixed with lipofectamine were added when cells were plated, followed by incubation for 72 h at 37 °C in 5 % CO_2-enriched air. Luc-Pair miR luciferase assay (GeneCopoeia) and FilterMax F5 microplate reader (Molecular Devices, Sunnyvale, CA) were used to analyze luciferase expression according to the manufacturer protocols.

Statistical analysis

The data are expressed as the mean ± SD of at least three independent experiments. The statistical analyses were carried out with Mann–Whitney *U* test for the comparison of medians. P value < 0.05 was considered to be significant.

Results

miRNA expression profile of DFSP

Initially, to determine which miRNAs were involved in the pathogenesis of DFSP, we performed miRNA PCR array analysis, consisting of 88 cancer-related miRNAs. A mixture of equal amounts of miRNAs from three normal skins and three DFSP tissues was prepared, and miRNA expression profile in each group was evaluated using the PCR array. Samples of dermatofibroma (DF), the benign fibrohistiocytic tumor, were also included in the analysis. There were several miRNAs increased or reduced in DFSP compared with DF and normal skin (Table 1). Among them, we focused on miR-205, because its expression was dramatically down-regulated in DFSP (3.54-cycle difference; 11.63-fold change in ΔΔCt method) but down-regulated in DF only slightly (1.60-cycle difference; 3.03-fold change in ΔΔCt method), compared with normal skin.

We tried to determine the localization of the miR-205 expression in normal skin tissues, DF tissues and DFSP tissues. In situ hybridization showed that miR-205 expression was evident in dermal fibroblasts of normal skin although hardly detected in tumor cells of DF or DFSP (Fig. 1a–f), consistent with the array data.

Table 1 Summary of microRNA expression in DFSP tissues by PCR array analysis

miRNA Name	DF-NS	DFSP-NS	miRNA Name	DF-NS	DFSP-NS
let-7a	0.05	0.8	miR-130a	1.73	−2.88
let-7b	1.34	1.87	miR-132	−0.19	−2.04
let-7c	−0.32	0.36	miR-133b	12.44	5.5
let-7d	1.11	1.64	miR-134	−2.07	−3.44
let-7e	0.48	1.16	miR-135b	0.27	1.15
let-7f	−0.39	−1.52	miR-138	5.33	0.18
let-7 g	0.21	−0.26	miR-140-5p	0.78	−1.4
let-7i	−0.12	−0.6	miR-142-5p	0.82	0.51
miR-1	5.1	2.92	miR-143	2.02	0.83
miR-7	−1.42	−0.85	miR-144	−0.01	−3.83
miR-9	−2.77	−6.35	miR-146a	1.54	2.84
miR-10a	−2.92	−2.36	miR-146b-5p	−1.02	−1.7
miR-10b	−1.77	−3.04	miR-148a	1.13	1.1
miR-15a	1.76	−0.75	miR-148b	0.17	−0.33
miR-15b	2.41	2.77	miR-149	1.61	2.1
miR-16	0.57	−0.92	miR-150	−0.01	1.33
miR-18a	−0.46	−0.47	miR-155	−0.65	3.62
miR-18b	0.48	1.03	miR-181a	0.59	−0.17
miR-19a	1.08	−0.5	miR-181b	−0.04	−0.05
miR-20a	1	0.36	miR-181c	−0.03	−0.82
miR-20b	1.02	−0.59	miR-181d	0.89	0.37
miR-21	−3.79	−2.4	miR-183	1.47	3.39
miR-23b	1.11	2.11	miR-184	0.52	4.24
miR-25	−1.05	−0.64	miR-191	0	−0.02
miR-27a	0.63	0.61	miR-193a-5p	0.31	1.53
miR-27b	0.5	0.22	miR-193b	1.27	2.4
miR-29a	1.27	0.27	miR-196a	−2.63	−2.46
miR-29b	−12.61	−14.71	miR-199a-3p	−1.14	−2.1
miR-30c	1.76	1.43	mir-200c	−0.32	3.63
miR-32	3.64	0.23	miR-203	0.14	3.81
miR-34a	−0.68	−1.57	miR-205	1.6	3.54
miR-34c-5p	−2.86	−2.28	miR-206	6.73	ND
miR-92a	0.17	1.91	miR-210	0.43	0.35
miR-96	1.8	2.86	miR-212	1.52	0.87
miR-98	−2.12	−1.92	miR-214	−0.33	0.51
miR-100	−0.14	−0.83	miR-215	−9.21	−10.66
miR-106a/17	0.65	−0.12	miR-218	0.08	−0.68
miR-122	3.1	−0.66	miR-222	0.31	0.1
miR-124	4.04	4.48	miR-301a	−0.81	−4.38
miR-125a-5p	0.08	0.9	mir-335	2.56	−1.48
miR-125b	−0.96	−2.16	miR-363	1.77	−3.59
miR-126	0.09	−0.62	miR-372	0.53	1.64
miR-127-5p	0.59	−0.39	miR-373	1.31	3.36
miR-128a	−0.4	−1.89	miR-378	1.25	1.24

A mixture of equal amounts of microRNAs from three normal skins (NS), three dermatofibroma (DF) sections or dermatofibrosarcoma protuberans (DFSP) sections was prepared, and microRNA expression profile in each group was evaluated using PCR array. The ΔΔCt (the raw Ct value of each microRNA−Ct value of small RNA housekeeping gene) was calculated. The difference of ΔΔCt between DF and NS or DFSP and NS was shown

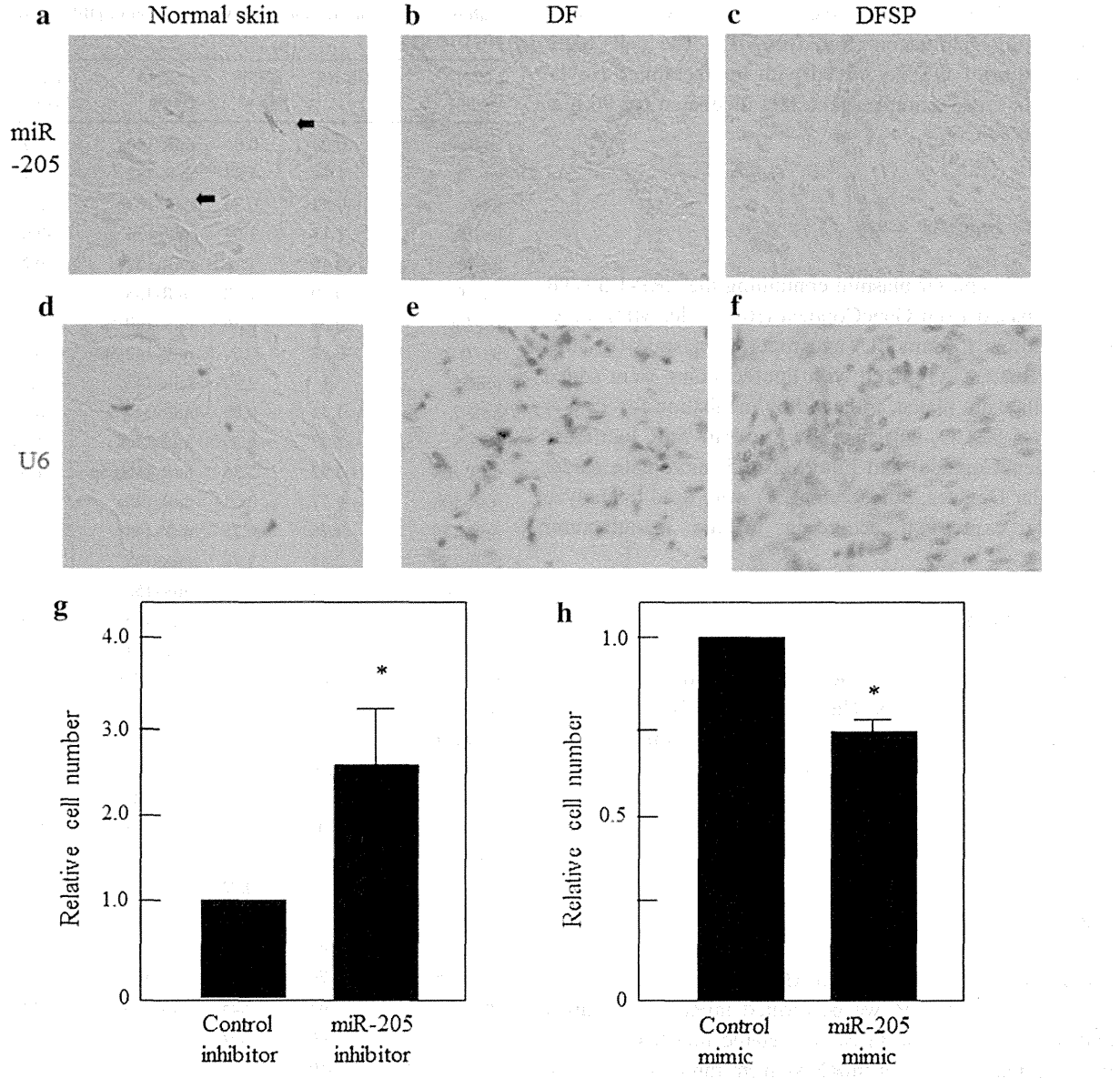

Fig. 1 **a–f** In vivo expression of miR-205 in normal skin (NS, **a**), dermatofibroma tissue (DF, **b**) and dermatofibrosarcoma protuberans tissue (DFSP, **c**) by in situ hybridization. U6 staining was also shown as the positive controls (**d–f**). Original magnification ×200. Nucleus was counterstained with nuclear fast red. *Black arrows* indicate dermal fibroblasts. The results of one experiment representative of three independent experiments are shown. (**g**) Normal fibroblasts were transfected with control or miR-205 inhibitor. After 72 h, the cell number was counted ($n = 3$). $^*P < 0.05$ as compared with the values in cells transfected with controls (1.0). (**h**) Cultured DFSP cells were transfected with control or miR-205 mimic. After 72 h, the cell number was counted ($n = 3$)

Next, to estimate the function of miR-205 in the pathogenesis of DFSP, miR-205 was inhibited by the specific inhibitor in cultured normal dermal fibroblasts, and the cell number was counted. As shown in Fig. 1g, transfection of the miR-205 inhibitor resulted in the significant up-regulation of cell number. In contrast, transfection of miR-205 mimic significantly decreased number of cultured DFSP cells (Fig. 1h). Taken together, miR-205 may contribute to the oncogenesis of DFSP by regulating cell proliferation.

miR-205 regulates LRP-1 expression

We tried to clarify the regulatory mechanisms by which miR-205 inhibits cell proliferation. We focused on low-density lipoprotein receptor-related protein 1 (LRP-1) as the putative target of miR-205, according to miRNA target gene predictions using TargetScan (version 6.2, http://www.targetscan.org/) and miRBase (http://www.mirbase.org/) [11]. LRP-1 is a large endocytic receptor that belongs to the low-density lipoprotein receptor family [12]. LRP-1 binds to and

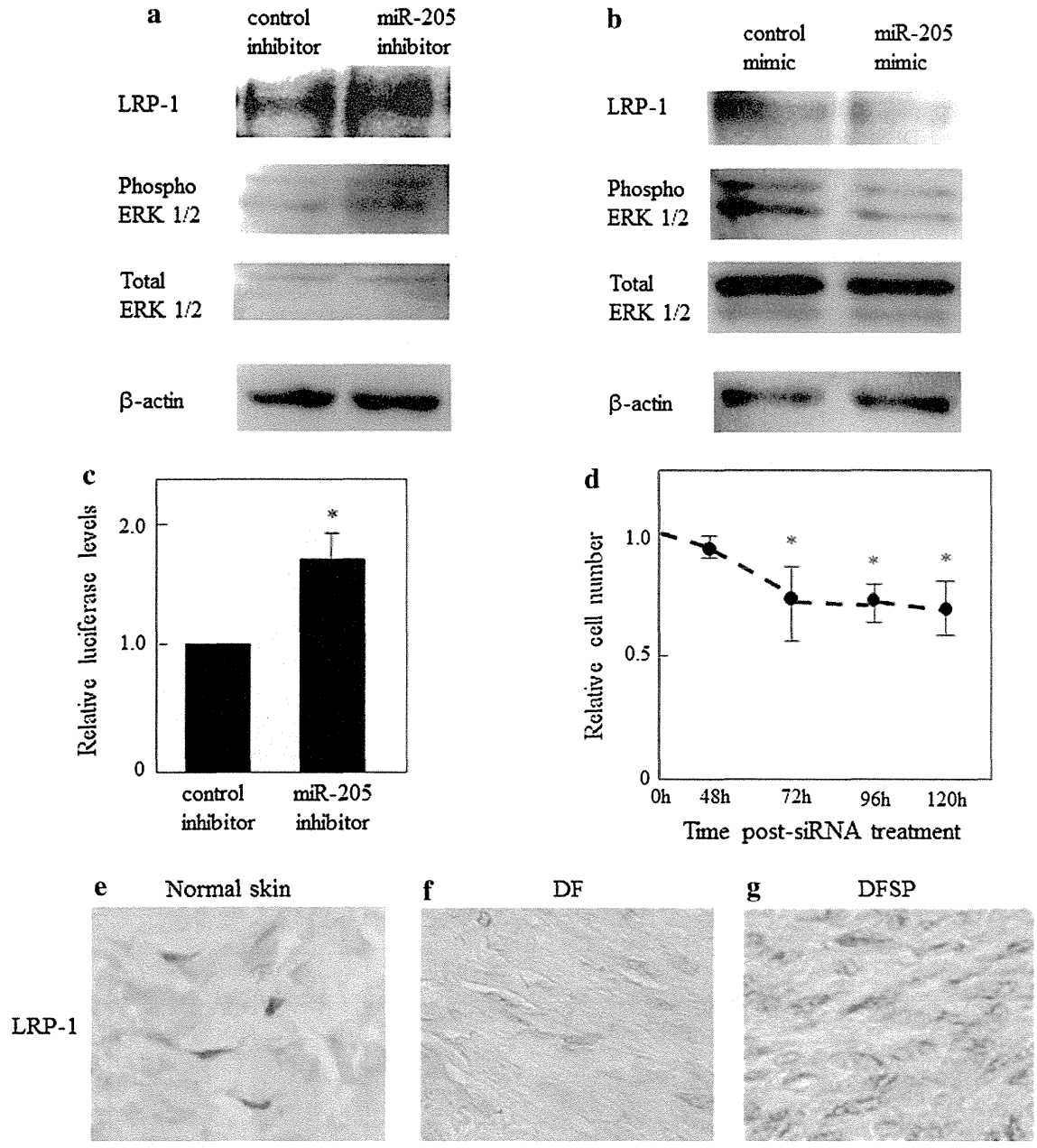

Fig. 2 **a** Normal dermal fibroblasts were transfected with control or miR-205 inhibitor for 72 h. Cell lysates were subjected to immunoblotting with antibodies for LRP-1, phosphorylated ERK1/2, total ERK1/2 and β-actin. The results of one experiment representative of three independent experiments are shown. **b** Cultured DFSP tumor cells were transfected with control or miR205 mimic. After 72 h, the expression of LRP-1, phosphorylated ERK1/2, total ERK1/2 and β-actin levels was analyzed by immunoblotting. The results of one experiment representative of three independent experiments are shown. **c** Normal human fibroblasts at a density of 1×10^4 cells/well in 96-well culture plates were transfected with luciferase reporter containing 3′UTR segment of LRP-1 and indicated miRNA inhibitors. The *bar graph* shows the relative luciferase activity ($n = 3$). $^*P < 0.05$ as compared with the values in cells with control inhibitor (1.0). **d** Cultured DFSP cells were treated with LRP-1 siRNA for 48, 72, 96 or 120 h. After incubation, the number of fibroblasts was counted ($n = 3$). $^*P < 0.05$ as compared with the values in control cells (1.0). **e–g** LRP-1 expression in normal skin (NS, **e**), dermatofibroma tissue (DF, f) and dermatofibrosarcoma protuberans tissue (DFSP, **g**). Paraffin sections were subjected to immunohistochemical analysis using antibody for LRP-1. Original magnification, ×400. The results of one experiment representative of three independent experiments are shown

endocytoses various ligands including proteases, protease-inhibitor complexes, macromolecular proteins and growth factors [6]. Several reports indicated the importance of LRP-1 in oncogenesis: LRP-1 promotes migration and invasion of human glioblastoma U87 cell lines [33], while LRP-1 silencing prevents the invasion of follicular thyroid cells [6].